

Spatial causal inference in the presence of preferential sampling to study the impacts of marine protected areas

Dongjae Son¹, Brian J. Reich¹, Erin M. Schliep¹, Shu Yang¹, and David A. Gill²

October 29, 2024

Abstract

Marine Protected Areas (MPAs) have been established globally to conserve marine resources. Given their maintenance costs and impact on commercial fishing, it is critical to evaluate their effectiveness to support future conservation. In this paper, we use data collected from the Australian coast to estimate the effect of MPAs on biodiversity. Environmental studies such as these are often observational, and processes of interest exhibit spatial dependence, which presents challenges in estimating the causal effects. Spatial data can also be subject to preferential sampling, where the sampling locations are related to the response variable, further complicating inference and prediction. To address these challenges, we propose a spatial causal inference method that simultaneously accounts for unmeasured spatial confounders in both the sampling process and the treatment allocation. We prove the identifiability of key parameters in the model and the consistency of the posterior distributions of those parameters. We show via simulation studies that the causal effect of interest can be reliably estimated under the proposed model. The proposed method is applied to assess the effect of MPAs on fish biomass. We find evidence of preferential sampling and that properly accounting for this source of bias impacts the estimate of the causal effect.

Key words: Poisson process; Potential outcomes; Propensity scores; Spatial confounding.

¹North Carolina State University

²Duke University

1 Introduction

Marine Protected Areas (MPAs) are spatially-demarcated areas of the ocean designated for the long-term conservation of marine biodiversity (IUCN, 2018). Given their broad application and rapid expansion globally ($\approx 8\%$ of the world's oceans), research interest on MPA effectiveness has also increased over the last two decades (Gill et al., 2019; UNEP-WCMC, 2018). For example, Edgar et al. (2014) assessed the impact of MPAs on fish population globally, and identified certain design attributes that seem to contribute to more positive effects (e.g. no-fishing or “no-take”, enforced, large, old, and isolated MPAs). Gill et al. (2017, 2024) synthesized a global database of ecological, socioeconomic, and management factors of MPAs to investigate whether MPAs are being effectively and equitably managed, and the effect of management on conservation impacts. They found that MPAs with adequate staff capacity and appropriate regulations had much greater positive impacts compared to others. Desbureaux et al. (2024) evaluated the impact of MPAs on fish productivity and local economy in coastal villages in Tanzania. They concluded that economic benefits can be found for MPAs whose productivity has declined.

Despite the large body of literature on MPA impacts, few studies employ causal inference methods to assess their effects. In a review of almost 200 MPA studies, Ferraro et al. (2019) found that very few studies accounted for confounding spatial and temporal factors that could bias impacts (e.g. placement bias). Since prohibiting fishing activities generates greater conservation outcomes (Grorud-Colvert et al., 2021) but could also have a negative effect of local communities (Kamat, 2014), scientific analyses of the effect on MPAs are important. This gives rise to the need to develop a spatial causal inference framework to properly assess policy efficacy.

Environmental studies such as analyses of MPA effects often rely on observational data to examine the effect of treatments or policies on ecological phenomena, as randomized trials are challenging to apply. Therefore, causal inference methods for observational studies are required to identify and estimate causal effects (Imbens and Rubin, 2015; Hernán and Robins, 2010). However, unlike various causal inference methods for independent data, ecological data often have spatial correlation. Spatial causal inference frameworks have recently been developed that account for spatial dependencies (Jarner et al., 2002; Davis et al., 2019; Schnell and Papadogeorgou, 2020;

Marques et al., 2022; Guan et al., 2023). These methods address unmeasured spatial confounders, which violate the key assumption in causal inference that there are no unmeasured confounders (Rubin, 1974, 1978) for observational studies. For example, Davis et al. (2019) estimate propensity scores using a spatial logistic regression with conditional autoregressive priors and use them to estimate the average treatment effect by augmented inverse propensity weighting. Schnell and Papadogeorgou (2020) propose a neighborhood adjustments method by spatial smoothing to mitigate the effect of unobserved spatial confounding. Guan et al. (2023) developed an approach using spectral representations to adjust for spatial confounders. For a more extensive review of existing spatial causal inference methods, see Reich et al. (2021).

In addition to spatial confounding, ecological data analyses are often complicated by preferential sampling. Preferential sampling refers to the situation where the selection of sampling locations is dependent on the spatial processes of interest (Pati et al., 2011; Diggle et al., 2010). For example, in our motivating MPA analysis, it may be that data are collected where they are easily accessible (e.g., close to the shoreline) where fish abundance might be low due to higher impacts from land-based activities including fishing (Campbell et al., 2020; Cinner et al., 2013). Preferential sampling has been shown to produce biases in parameter estimation or spatial prediction (Diggle et al., 2010; Pati et al., 2011; Gelfand et al., 2012; Schliep et al., 2023). Diggle et al. (2010) proposed the foundational geostatistical model that accounts for preferential sampling using a shared spatial random effect between a response model and a point process model. Pati et al. (2011) proposed a Bayesian hierarchical model for which there is a theoretical guarantee that the posterior distributions of the model parameters are consistent and a proper posterior can be derived for the parameters regarding the degree of preferential sampling. Gelfand et al. (2012) proposed a simulation-based approach to assess the effect of preferential sampling on spatial prediction. Schliep et al. (2023) proposed a weighted composite likelihood approach for estimating spatial covariance parameters under preferential sampling when the focus is on spatial prediction.

To our knowledge, there does not exist a spatial causal inference method that mitigates the effect of preferential sampling bias common in environmental studies. In this paper, we introduce a novel approach to spatial causal inference that accounts for preferential sampling bias. Motivated

by Diggle et al. (2010) and Pati et al. (2011), we specify log-Gaussian Cox processes to model point patterns of sampling locations, which are connected to potential outcome models through shared latent spatial processes. Assuming a binary policy, two policy groups have varying degrees of preferential sampling. By modeling the sampling intensities for each policy group, we can also calculate propensity scores by using the result from superposition of Poisson processes (Durrett, 1999). In this way, we can specify a spatial causal inference model that accounts for preferential sampling in a unified hierarchical model. We present theoretical results related to the identifiability of the parameters of interest and weak consistency of the posterior distribution.

The proposed method is applied to the MPA data presented in Gill et al. (2024) with focus on Australia. The Australian marine jurisdictional area is notable for its diverse and distinctive range of species and habitats (Knowles et al., 2015). MPAs have been established to protect such ecological and economic resources. Across this spatial domain, we investigate the causal effect of MPAs on fish biomass by comparing MPAs and non-MPAs.

The rest of the paper is composed as follows. In Section 2, we introduce the proposed model for the spatial causal inference that accounts for preferential sampling along with the computational details for feasibility. We also define the causal effect of interest and the necessary assumptions for identification. In Section 3, theoretical results are presented, which includes the identification of model parameters and posterior consistency. In Section 4, an extensive simulation study is presented to assess the performance of the proposed model. In Section 5, we apply the model to the fish biomass data and examine the effect of the MPAs. In Section 6, concluding remarks are given.

2 Statistical methods

2.1 A potential outcome approach and definition of the causal effect

We propose a hierarchical modeling framework for spatial causal inference in the presence of preferential sampling. Denote the spatial domain of interest as $\mathcal{D} \subseteq \mathbb{R}^2$. There exist two policies, denoted $a = 0$ and $a = 1$ which in the MPA analysis represent no protection and protection

policies, respectively. We specify the response model in terms of potential outcomes (Rubin, 1974). Denote $Y_a(\mathbf{s})$ as the potential outcome under policy $a \in \{0, 1\}$ at spatial location $\mathbf{s} \in \mathcal{D}$. Then the potential outcome model for each policy is

$$Y_a(\mathbf{s}) = \alpha_a + \mathbf{X}(\mathbf{s})^\top \boldsymbol{\beta}_a + U_a(\mathbf{s}) + \epsilon_a(\mathbf{s}), \quad (1)$$

where α_a is an intercept, $\mathbf{X}(\mathbf{s})$ is a p -dimensional covariate vector, $\boldsymbol{\beta}_a \in \mathbb{R}^p$ is a vector of regression coefficients, $\mathbf{U}(\mathbf{s}) = (U_0(\mathbf{s}), U_1(\mathbf{s}))^\top$ is a mean-zero bivariate Gaussian process which might contain unmeasured spatial confounders and post-treatment processes, and $\epsilon_a(\mathbf{s})$ is a measurement error term distributed normally with mean zero and variance τ_a^2 , independent of $U_a(\mathbf{s})$.

The estimands of interest are the local and average causal effects. The local causal effect is

$$\Delta(\mathbf{s}) = \alpha_1 - \alpha_0 + \mathbf{X}(\mathbf{s})^\top (\boldsymbol{\beta}_1 - \boldsymbol{\beta}_0) + U_1(\mathbf{s}) - U_0(\mathbf{s}). \quad (2)$$

The average causal effect, referred to as the average policy effect (APE) is

$$\Delta = |\mathcal{D}|^{-1} \int_{\mathcal{D}} \Delta(\mathbf{s}) d\mathbf{s}. \quad (3)$$

To account for possible preferential sampling, we model the measurement locations using spatial point processes. Let \mathcal{S}_a be the set of n_a sampling locations given policy a for $a \in \{0, 1\}$. A natural model for \mathcal{S}_a is the doubly stochastic inhomogeneous Poisson point process (Pati et al., 2011) with log intensity

$$\log \{\lambda_a(\mathbf{s})\} = \eta_a^* + \mathbf{X}(\mathbf{s})^\top \boldsymbol{\delta}_a^* + V_a(\mathbf{s}) + \phi_a \{\alpha_a + \mathbf{X}(\mathbf{s})^\top \boldsymbol{\beta}_a + U_a(\mathbf{s})\}, \quad (4)$$

where η_a^* is an intercept, $\boldsymbol{\delta}_a^* \in \mathbb{R}^p$ is a regression coefficient vector for each intensity model, and $\mathbf{V}(\mathbf{s}) = (V_0(\mathbf{s}), V_1(\mathbf{s}))^\top$ is a mean-zero bivariate Gaussian process, which is independent of $\mathbf{U}(\mathbf{s})$. By incorporating $\alpha_a + \mathbf{X}(\mathbf{s})^\top \boldsymbol{\beta}_a + U_a(\mathbf{s})$ from (1) in the intensity function, we allow for preferential sampling. That is, if $\phi_a > 0$, the sites with larger mean response are more likely to be sampled. Under this formulation, the sampling locations under both policies follow log Gaussian

Cox processes (Møller et al., 1998; Banerjee et al., 2003).

In this hierarchical model, $U_0(\mathbf{s})$ and $U_1(\mathbf{s})$ are shared latent processes between potential outcome models and point process models (Diggle et al., 2010) to adjust for preferentially sampled locations, and ϕ_0 and ϕ_1 are coefficients to determine the degree of preferential sampling under policies 0 and 1, respectively. Under this model specification, the sampling locations are non-ignorable in computing the APE in (3) due to the shared processes $U_0(\mathbf{s})$ and $U_1(\mathbf{s})$. The processes $V_0(\cdot)$ and $V_1(\cdot)$ are residual spatial processes to capture spatial trends within each point process that is not explained by the covariates and shared processes.

We can reparametrize (4) by setting $\eta_a = \eta_a^* + \phi_a \alpha_a$ and $\boldsymbol{\delta}_a = \boldsymbol{\delta}_a^* + \phi_a \boldsymbol{\beta}_a$ and specify the models for the point processes as

$$\log \{\lambda_a(\mathbf{s})\} = \eta_a + \mathbf{X}(\mathbf{s})^\top \boldsymbol{\delta}_a + V_a(\mathbf{s}) + \phi_a U_a(\mathbf{s}) + \psi_a(\mathbf{s}). \quad (5)$$

Given this specification, location densities $\lambda_a(\mathbf{s}) / \int_{\mathcal{D}} \lambda_a(\mathbf{w}) d\mathbf{w}$ are written as

$$p_a(\mathbf{s} | \mathcal{X}, \mathcal{U}_a, \mathcal{V}_a) = \frac{\exp \{\mathbf{X}(\mathbf{s})^\top \boldsymbol{\delta}_a + V_a(\mathbf{s}) + \phi_a U_a(\mathbf{s})\}}{\int_{\mathcal{D}} \exp \{\mathbf{X}(\mathbf{w})^\top \boldsymbol{\delta}_a + V_a(\mathbf{w}) + \phi_a U_a(\mathbf{w})\} d\mathbf{w}} \quad (6)$$

for $a \in \{0, 1\}$, where $\mathcal{X} = \{\mathbf{X}(\mathbf{s}) : \mathbf{s} \in \mathcal{D}\}$, $\mathcal{U}_a = \{U_a(\mathbf{s}) : \mathbf{s} \in \mathcal{D}\}$, and $\mathcal{V}_a = \{V_a(\mathbf{s}) : \mathbf{s} \in \mathcal{D}\}$. Furthermore, let $A(\mathbf{s})$ denote the policy indicator such that $A(\mathbf{s}) = 1$ if location \mathbf{s} is assigned policy $a = 1$ and $A(\mathbf{s}) = 0$ if assigned policy $a = 0$. By superposition of two Poisson processes (Durrett, 1999), given that a sample is taken at \mathbf{s} , the probability of policy assignment mechanism conditioned on $\mathbf{X}(\mathbf{s})$, $\mathbf{U}(\mathbf{s})$, and $\mathbf{V}(\mathbf{s})$ is

$$\mathbb{P}\{A(\mathbf{s}) = 1 | \mathbf{X}(\mathbf{s}), \mathbf{U}(\mathbf{s}), \mathbf{V}(\mathbf{s})\} = \frac{\lambda_1(\mathbf{s})}{\lambda_0(\mathbf{s}) + \lambda_1(\mathbf{s})} = \text{expit}\{\mathbf{D}(\mathbf{s})\}, \quad (7)$$

where $\text{expit}(\cdot)$ is a sigmoid function and

$$\mathbf{D}(\mathbf{s}) = \eta_1 - \eta_0 + \mathbf{X}(\mathbf{s})^\top (\boldsymbol{\delta}_1 - \boldsymbol{\delta}_0) + \{V_1(\mathbf{s}) + \phi_1 U_1(\mathbf{s})\} - \{V_0(\mathbf{s}) + \phi_0 U_0(\mathbf{s})\}.$$

The probability defined in (7) is the propensity score (Rosenbaum and Rubin, 1983).

Turning to the modeling of the bivariate spatial random effects, we employ a linear model of coregionalization (LMC) (Banerjee et al., 2003). Define $\tilde{U}_a(\mathbf{s})$ for $a \in \{0, 1\}$ as independent Gaussian processes with Matérn covariance function $\sigma_{u,a}^2 \mathcal{R}(h; \rho_u, \kappa_u)$ (Williams and Rasmussen, 2006), where $h = \|\mathbf{s} - \mathbf{s}'\|$ for $\mathbf{s}, \mathbf{s}' \in \mathcal{D}$, $\rho_u > 0$ is a spatial dependence parameter, $\kappa_u > 0$ is a smoothness parameter, and

$$\mathcal{R}(h; \rho_u, \kappa_u) = \frac{1}{2^{\kappa_u-1} \Gamma(\kappa_u)} \left(\frac{h}{\rho_u}\right)^{\kappa_u} \mathcal{K}_{\kappa_u} \left(\frac{h}{\rho_u}\right). \quad (8)$$

Here, \mathcal{K}_{κ_u} denotes the modified Bessel function of the second kind. A special case of $\mathcal{R}(h; \rho_u, \kappa_u)$ is an exponential correlation $\mathcal{R}(h; \rho_u) = \exp(-h/\rho_u)$ with $\kappa_u = 1/2$. Then, using the LMC, we have

$$U_0(\mathbf{s}) = \tilde{U}_0(\mathbf{s}) \quad \text{and} \quad U_1(\mathbf{s}) = \tilde{U}_1(\mathbf{s}) + \gamma_u \tilde{U}_0(\mathbf{s})$$

for all $\mathbf{s} \in \mathcal{D}$. The bivariate spatial processes $V_0(\mathbf{s})$ and $V_1(\mathbf{s})$ are modeled analogously.

To understand the consequences of preferential sampling, we evaluate the expectation of $Y_1(\mathbf{s}) - Y_0(\mathbf{s})$ averaging over both the spatial location and potential outcomes, conditionally on \mathcal{X} . Appendix A shows that

$$\mathbb{E}\{Y_1(\mathbf{s}) - Y_0(\mathbf{s})\} \approx (\alpha_1 - \alpha_0) + (\bar{\mathbf{X}}_1^\top \boldsymbol{\beta}_1 - \bar{\mathbf{X}}_0^\top \boldsymbol{\beta}_0) + [\phi_1 \text{Var}\{U_1(\mathbf{s})\} - \phi_0 \text{Var}\{U_0(\mathbf{s})\}], \quad (9)$$

where $\bar{\mathbf{X}}_a = \int_{\mathcal{D}} \mathbf{X}(\mathbf{w}) \exp\{\mathbf{X}(\mathbf{w})^\top \boldsymbol{\delta}_a\} d\mathbf{w} / \int_{\mathcal{D}} \exp\{\mathbf{X}(\mathbf{w})^\top \boldsymbol{\delta}_a\} d\mathbf{w}$, and the variances of the stationary processes are $\text{Var}\{U_1(\mathbf{s})\} = \sigma_{u,1}^2 + \gamma_u^2 \sigma_{u,0}^2$ and $\text{Var}\{U_0(\mathbf{s})\} = \sigma_{u,0}^2$. The second term shows how preferential sampling affects the covariate distribution in the two treatment groups. The third term quantifies the effects of preferential sampling that cannot be explained by covariates. When $\text{Var}\{U_0(\mathbf{s})\} = \text{Var}\{U_1(\mathbf{s})\} = 0$ or $\phi_0 = \phi_1 = 0$, this term is zero, meaning the underlying spatial processes are deterministic or the sampling intensities do not depend on the response. This expression also suggests that the effects of preferential sampling are the most prominent when the sampling protocols differ by treatment group, e.g., if $\text{Var}(U_0) = \text{Var}(U_1)$ then the term is proportional to $\phi_1 - \phi_0$, and so the term is nonzero only if the strength of preferential sampling differs by

treatment group.

The fundamental problem of causal inference is that at most one of the potential outcomes is observed at location \mathbf{s} . This implies that both $Y_0(\mathbf{s})$ and $Y_1(\mathbf{s})$ are not simultaneously observable and leads us to view causal inference as a missing data problem (Ding and Li, 2018). Furthermore, since the location sampling processes are confounded by the underlying spatial processes, we require additional assumptions to identify (3). These directly follow or slightly modify the common assumptions in causal inference (Rubin, 1978; Rosenbaum and Rubin, 1983). Let us define $\mathcal{U} = (\mathcal{U}_0, \mathcal{U}_1)$, $\mathcal{V} = (\mathcal{V}_0, \mathcal{V}_1)$, and $\mathcal{Y}_a = \{Y_a(\mathbf{s}) : \mathbf{s} \in \mathcal{D}\}$ for $a \in \{0, 1\}$. For all $\mathbf{s} \in \mathcal{D}$,

Assumption 1. *Stable Unit Treatment Values (SUTVA):* For an observed outcome $Y(\mathbf{s})$ and a treatment indicator $A(\mathbf{s})$, $Y(\mathbf{s}) = Y_0(\mathbf{s}) \{1 - A(\mathbf{s})\} + Y_1(\mathbf{s})A(\mathbf{s})$.

Assumption 2. *Latent ignorability:* $\mathcal{S}_0, \mathcal{S}_1 \perp\!\!\!\perp \mathcal{Y}_0, \mathcal{Y}_1$ given $\mathcal{X}, \mathcal{U}, \mathcal{V}$.

Assumption 3. *Positive intensity:* $\lambda_a(\mathbf{s}) > 0$ almost surely for all $\mathbf{s} \in \mathcal{D}$ and $a \in \{0, 1\}$.

Assumption 1 states that “there is no interference and there is only a single version of treatment” (Rubin, 1978). Assumption 2 implies that the propensity score given \mathcal{X}, \mathcal{U} , and \mathcal{V} does not depend on \mathcal{Y}_0 and \mathcal{Y}_1 given $\mathbf{X}(\mathbf{s}), \mathbf{U}(\mathbf{s})$ and $\mathbf{V}(\mathbf{s})$, i.e.,

$$\mathbb{P}\{A(\mathbf{s}) = 1 | \mathcal{X}, \mathcal{U}, \mathcal{V}, \mathcal{Y}_0, \mathcal{Y}_1\} = \mathbb{P}\{A(\mathbf{s}) = 1 | \mathbf{X}(\mathbf{s}), \mathbf{U}(\mathbf{s}), \mathbf{V}(\mathbf{s})\}$$

by the relationship (7). Subsequently, $\{Y_0(\mathbf{s}), Y_1(\mathbf{s})\}$ is conditionally independent of $A(\mathbf{s})$. Assumption 3 implies that

$$\mathbb{P}\{A(\mathbf{s}) = 1 | \mathbf{X}(\mathbf{s}), \mathbf{U}(\mathbf{s}), \mathbf{V}(\mathbf{s})\} = \frac{\lambda_1(\mathbf{s})}{\lambda_0(\mathbf{s}) + \lambda_1(\mathbf{s})} \in (0, 1)$$

almost surely for all $\mathbf{s} \in \mathcal{D}$. This means that both treatments are possible for all $\mathbf{s} \in \mathcal{D}$, which enables us to estimate the local causal effects.

2.2 Computational methodology

We propose a fully Bayesian analysis via Markov Chain Monte Carlo (MCMC) to estimate Δ and its uncertainty. Computation is complicated by the stochastic integration in (6). In Section 2.2.1, we describe a discretized model to approximate this integration, and in Section 2.2.2, we provide MCMC details to fit this discretized model.

2.2.1 Grid approximation

The proposed model consists of stochastic integrals making computation challenging. As such, numerical integration using grid cells is employed (Diggle et al., 2010; Pati et al., 2011; Gelfand and Schliep, 2018). We partition the domain into G equally-sized grid cells, i.e., $\mathcal{D} = \cup_{g=1}^G \mathcal{D}_g$ with $|\mathcal{D}_g| = \frac{|\mathcal{D}|}{G}$ for all $g = 1, \dots, G$, and approximate the integral as

$$\int_{\mathcal{D}} \exp \{ \mathbf{X}(\mathbf{s})^\top \boldsymbol{\delta}_a + V_a(\mathbf{s}) + \phi_a U_a(\mathbf{s}) \} ds \approx \frac{|\mathcal{D}|}{G} \sum_{g=1}^G \exp (\mathbf{X}_g^\top \boldsymbol{\delta}_a + V_{a,g} + \phi_a U_{a,g}) \quad (10)$$

for $a \in \{0, 1\}$. In (10), \mathbf{X}_g , $U_{a,g}$ and $V_{a,g}$ are grid-level values of $\mathbf{X}(\mathbf{s})$, $U_a(\mathbf{s})$, and $V_a(\mathbf{s})$ evaluated at the centroid of the g^{th} grid cell \mathbf{c}_g , i.e., $\mathbf{X}_g = \mathbf{X}(\mathbf{c}_g)$ and similarly for $U_{a,g}$ and $V_{a,g}$. This implies that the spatial random effects and the covariates representing each grid cell are assumed to be constant in each grid cell.

By using the LMC and the property of Gaussian processes that any finite collection of them follows a multivariate normal distribution (MVN), we have

$$U_{0,g} = \tilde{U}_{0,g} \quad \text{and} \quad U_{1,g} = \tilde{U}_{1,g} + \gamma_u \tilde{U}_{0,g}$$

for $g = 1, \dots, G$ where $\tilde{\mathbf{U}}_a = \left(\tilde{U}_{a,1}, \dots, \tilde{U}_{a,G} \right)^\top$ is distributed as

$$\tilde{\mathbf{U}}_a \sim \text{MVN} \{ \mathbf{0}_G, \sigma_{u,a}^2 \mathbf{R}(\rho_u, \kappa_u) \}. \quad (11)$$

Here, $\mathbf{0}_G$ is a zero vector of length G and $\mathbf{R}(\rho_u, \kappa_u)$ is a correlation matrix with its diagonal entries

being 1 and off-diagonal elements corresponding to $\mathcal{R}(\|\mathbf{c}_g - \mathbf{c}_{g'}\|; \rho_u, \kappa_u)$ for $g, g' \in \{1, \dots, G\}$. Using a similar argument, $V_{0,g}$ and $V_{1,g}$ can be modeled by $V_{0,g} = \tilde{V}_{0,g}$ and $V_{1,g} = \tilde{V}_{1,g} + \gamma_v \tilde{V}_{0,g}$ for $g = 1, \dots, G$, where $\tilde{\mathbf{V}}_a \sim \text{MVN}\{\mathbf{0}_G, \sigma_{v,a}^2 \mathbf{R}(\rho_v, \kappa_v)\}$ for $a \in \{0, 1\}$.

Given the spatial random effects, the number of observations within each grid cell follows a Poisson distribution. The hierarchical model is written as

$$Y_0(\mathbf{s}) = \alpha_0 + \mathbf{X}(\mathbf{s})^\top \boldsymbol{\beta}_0 + \tilde{U}_{0,g(\mathbf{s})} + \epsilon_0(\mathbf{s}) \quad (12)$$

$$Y_1(\mathbf{s}) = \alpha_1 + \mathbf{X}(\mathbf{s})^\top \boldsymbol{\beta}_1 + \tilde{U}_{1,g(\mathbf{s})} + \gamma_u \tilde{U}_{0,g(\mathbf{s})} + \epsilon_1(\mathbf{s}) \quad (13)$$

$$N_{0,g} \sim \text{Poisson}(|\mathcal{D}_g| \cdot \lambda_{0,g}) \quad (14)$$

$$N_{1,g} \sim \text{Poisson}(|\mathcal{D}_g| \cdot \lambda_{1,g}) \quad (15)$$

$$\log\{\lambda_{0,g}\} = \eta_0 + \mathbf{X}_g^\top \boldsymbol{\delta}_0 + \tilde{V}_{0,g} + \phi_0 \tilde{U}_{0,g} + \psi_{0,g} \quad (16)$$

$$\log\{\lambda_{1,g}\} = \eta_1 + \mathbf{X}_g^\top \boldsymbol{\delta}_1 + \tilde{V}_{1,g} + \gamma_v \tilde{V}_{0,g} + \phi_1 (\tilde{U}_{1,g} + \gamma_u \tilde{U}_{0,g}) + \psi_{1,g} \quad (17)$$

for $g = 1, \dots, G$, where $g(\mathbf{s})$ is the index of the grid where \mathbf{s} lies, i.e., $g(\mathbf{s}) = k$ for some $k \in \{1, \dots, G\}$ if $\mathbf{s} \in \mathcal{D}_k$. Here, $N_{a,g}$ is the number of observations in g which received treatment $a \in \{0, 1\}$, and $\psi_{a,g}$ is an additional random effect component for explaining nonspatial heterogeneity, which is independently distributed as $\text{Normal}(0, \tau_{\psi_a}^2)$. Note that $\sum_{g=1}^G N_{a,g} = n_a$ is the total number of samples taken at locations under policy a , and $n_0 + n_1 = n$ is the sample size.

The APE, Δ , over the domain is approximated by

$$\Delta \approx G^{-1} \sum_{g=1}^G \Delta_g, \quad (18)$$

where $\Delta_g = \alpha_1 - \alpha_0 + \mathbf{X}_g^\top (\boldsymbol{\beta}_1 - \boldsymbol{\beta}_0) + U_{1,g} - U_{0,g}$ is a local causal effect at grid cell \mathcal{D}_g . If the grid cell sizes vary, (18) can be modified by applying weights. The propensity score at \mathcal{D}_g is approximated as

$$\frac{\lambda_{1,g}}{\lambda_{0,g} + \lambda_{1,g}} = \text{expit}\{\eta_1 - \eta_0 + \mathbf{X}_g^\top (\boldsymbol{\delta}_1 - \boldsymbol{\delta}_0) + (V_{1,g} + \phi_1 U_{1,g}) - (V_{0,g} + \phi_1 U_{0,g})\}. \quad (19)$$

2.2.2 MCMC details

Model inference is obtained in a Bayesian framework. We assign proper conjugate Gaussian priors for α_a , β_a , η_a , and δ_a for $a \in \{0, 1\}$. Normal conjugate priors are assigned to the parameters controlling the degree of preferential sampling and to the parameters of the LMC. Inverse-gamma priors are assigned to the variance components τ_a^2 , $\sigma_{u,a}^2$, $\sigma_{v,a}^2$, and $\tau_{\psi_a}^2$ for $a \in \{0, 1\}$. We assign proper priors to the spatial dependence parameters and the smoothness parameters ρ_u , ρ_v , κ_u and κ_v . The spatial random effects $\tilde{\mathbf{U}}_a$ and $\tilde{\mathbf{V}}_a$ are modeled using the Gaussian processes as described in Section 2.2.1.

Bayesian inference of the parameters and hyperparameters for the models (12)-(17) is obtained using MCMC. The model parameters and hyperparameters are sampled using a mixture of Gibbs sampling, Metropolis random walk, and Hamiltonian Monte Carlo (HMC) sampling (Neal et al., 2011). Missing potential outcomes are imputed using the predictive distributions (12) and (13) at every step of MCMC. The log intensities are updated by HMC, while the covariance hyperparameters ρ_u , ρ_v , κ_u and κ_v are updated via Metropolis random walk. All the remaining parameters are updated by Gibbs samplers. The details of the MCMC algorithm can be found in the Appendix.

3 Theoretical properties of the proposed model

In this section, we establish the theoretical properties of the proposed method. We first declare additional notation and assumptions. We define $\boldsymbol{\theta} = (\boldsymbol{\theta}_{\mathcal{M}}^\top, \boldsymbol{\theta}_{\mathcal{C}}^\top)^\top$ where

$$\boldsymbol{\theta}_{\mathcal{M}} = \{\alpha_0, \boldsymbol{\beta}_0, \boldsymbol{\delta}_0, \eta_0, \phi_0, \tau_0, \alpha_1, \boldsymbol{\beta}_1, \eta_1, \boldsymbol{\delta}_1, \phi_1, \tau_1, \gamma_u, \gamma_v\} \quad (20)$$

is the vector of parameters of interest and

$$\boldsymbol{\theta}_{\mathcal{C}} = \{\rho_u, \rho_v, \kappa_u, \kappa_v, \sigma_{u,0}^2, \sigma_{u,1}^2, \sigma_{v,0}^2, \sigma_{v,1}^2\} \quad (21)$$

represents the vector of hyperparameters. Additionally, we define

$$\mathcal{W} = \left\{ \left(\tilde{U}_a(\mathbf{s}), \tilde{V}_a(\mathbf{s}) \right) : \mathbf{s} \in \mathcal{D}, a \in \{0, 1\} \right\}. \quad (22)$$

The theorems require the following assumptions.

Assumption 4. *The prior density for $\boldsymbol{\theta}_{\mathcal{M}}$ is positive for all possible values of $\boldsymbol{\theta}_{\mathcal{M}}$. Further, the prior for κ_u satisfies $\mathbb{P}\{\kappa_u \geq 1/2\} > 0$ (similarly for κ_v), while proper priors are assigned to ρ_u , ρ_v , $\sigma_{u,a}^2$ and $\sigma_{v,a}^2$ for $a \in \{0, 1\}$.*

Assumption 5. *The matrices \mathbf{X}_S with i^{th} row corresponding to $\mathbf{X}(\mathbf{s}_i)$ and \mathbf{X}_G with k^{th} row corresponding to $\mathbf{X}(\mathbf{c}_k)$ are full rank.*

Assumption 6. *$\mathbf{X}(\mathbf{s})$ is uniformly bounded, i.e., there exists $C > 0$ such that $\|\mathbf{X}(\mathbf{s})\| \leq C$ for all $\mathbf{s} \in \mathcal{D}$.*

Finally, the following theorems hold.

Theorem 1. *Under models (12) – (17) and Assumptions 1 – 3 and 5, the vector of parameters $\boldsymbol{\theta}$ is identifiable.*

Theorem 2. *Under the models (1) and (5), and Assumptions 1 – 4, and 6, the posterior distribution of $\boldsymbol{\omega} = (\boldsymbol{\theta}_{\mathcal{M}}, \mathcal{W})$ is weakly consistent.*

Theorem 1 guarantees that the model parameters are identifiable without any information from the prior distributions for $\boldsymbol{\theta}$. In particular, we can identify the correlation between potential outcomes at the same location by leveraging spatial dependence which is not possible for non-spatial models. Theorem 2 states that within a class of prior distributions for $\boldsymbol{\theta}_{\mathcal{M}}$ and \mathcal{W} , the posterior converges to the true distribution in a weak sense, which implies that $\Delta(\mathbf{s})$ and Δ are estimable. Refer to Ghosh and Ramamoorthi (2003) or Ghosal and Van der Vaart (2017) for a formal definition of weak consistency in detail. Proofs are given in Appendix.

4 Simulation study

In this section, we conduct simulation studies to illustrate the bias caused by ignoring preferential sampling and the ability of the proposed method to mitigate this bias. We compare the performance of the proposed hierarchical model (“full”) with the model that only considers the response layers (12) and (13) and thus ignores preferential sampling (“naive”).

4.1 Data generation process

The domain of interest is $\mathcal{D} = [0, 1]^2$, which we discretize into 20×20 square grid cells. The data generation is based on the model defined by (12) – (17). We generate $p = 2$ independent covariates from Gaussian processes with exponential covariance kernel whose variance is 0.5 and spatial dependence parameter is 0.05, to construct \mathbf{X}_g for $g = 1, \dots, G = 20^2$.

We consider eight different scenarios to compare the two models. The first six scenarios differ based on (i) degree of preferential sampling, (ii) spatial dependence, and (iii) the expected number of observations. The last two scenarios consider nonstationarity and non-Gaussian data. Specific details for each scenario are given in Table 1. In each scenario, we set $\alpha_0 = 2$, $\alpha_1 = 4$, $\beta_0 = (1, 1)^\top$, $\beta_1 = (-1, -1)^\top$, $\delta_0^* = (1, 1)^\top$ and $\delta_1^* = (-1, -1)^\top$. Spatial random fields are generated by Gaussian processes with exponential covariance functions so that $\tilde{\mathbf{U}}_a$ and $\tilde{\mathbf{V}}_a$ are distributed as $\text{MVN}\{\mathbf{0}_G, \sigma^2 \mathbf{R}(\rho)\}$ where (g, g') entry of $\mathbf{R}(\rho)$ is $\exp(-\|\mathbf{c}_g - \mathbf{c}_{g'}\|/\rho)$, $\sigma^2 = 1$ and $\rho \in \{0.1, 0.2\}$ for $g, g' \in \{1, \dots, 20^2\}$. The LMC parameters are set to $\gamma_u = -0.5$ and $\gamma_v = 0.5$. The degrees of preferential sampling are set to be $\phi_0 = \phi$ and $\phi_1 = 1.5\phi$, where $\phi \in \{0, 1/3, 2/3, 1\}$, with $\phi = 0$ signifying nonpreferential sampling and $\phi = 1$ signifying strong preferential sampling. Recall from (4) that $\delta_a = \delta_a^* + \phi_a \beta_a$ varies with ϕ_a . The variances are all set to $\tau_0^2 = \tau_1^2 = \tau_{\psi_0}^2 = \tau_{\psi_1}^2 = 0.1$. The number of observations in each grid cell, $N_{0,g}$ and $N_{1,g}$, are generated from Poisson distributions where the mean intensities $\lambda^* = G^{-1} \sum_{g=1}^G \lambda_{a,g}$ are set to $\lambda^* \in \{5, 10\}$. This is achieved by controlling the values of η_0 and η_1 for each simulation set. These values result in 4,000 observations, on average, when $\lambda^* = 5$, and 8,000 observations, on average, when $\lambda^* = 10$. The realizations of the Poisson process on each grid cell represent the number of observations located in the grid cell. We set the covariates of each observation to have the same values as those

of the grid cell in which the site is located. We present six scenarios by varying these parameters as specified in Table 1.

To examine robustness to model misspecification, Scenarios 7 and 8 generate spatial processes that are nonstationary and non-Gaussian, respectively. The grid cell centroids with the y -coordinates being squared are used to generate nonstationary \mathbf{V}_0 and \mathbf{V}_1 (scenario 7). To incorporate non-Gaussianity (scenario 8), the log intensities of the following forms

$$\log \{\lambda_{0,g}\} = \eta_0 + \mathbf{X}_g^\top \boldsymbol{\delta}_0 + V_{0,g} + \phi_0 \left\{ U_{0,g} \mathbb{I}(U_{0,g} > 0) - \sqrt{\frac{\sigma^2}{2\pi}} \right\} + \psi_{0,g}$$

and

$$\log \{\lambda_{1,g}\} = \eta_1 + \mathbf{X}_g^\top \boldsymbol{\delta}_1 + V_{1,g} + \phi_1 \left\{ U_{1,g} \mathbb{I}(U_{1,g} > 0) - \sqrt{\frac{(1 + \gamma_u^2)\sigma^2}{2\pi}} \right\} + \psi_{1,g}$$

are considered to introduce the effect of \mathbf{U}_0 and \mathbf{U}_1 on the point processes after non-Gaussian transformations.

We assign proper priors $\alpha_a \sim \text{Normal}(0, 10^2)$, $\boldsymbol{\beta}_a \sim \text{MVN}(\mathbf{0}_2, 10^2 \mathbb{I}_2)$, $\eta_a \sim \text{Normal}(0, 10^2)$, and $\boldsymbol{\delta}_a \sim \text{MVN}(\mathbf{0}_2, 10^2 \mathbb{I}_2)$ for $a \in \{0, 1\}$. The LMC parameters, γ_u and γ_v , and the parameters governing preferential sampling, ϕ_0 and ϕ_1 , are assigned independent $\text{Normal}(0, 10^2)$. The variance components τ_a^2 , $\sigma_{u,a}^2$, $\sigma_{v,a}^2$, and $\tau_{\psi_a}^2$ are assigned with Inverse-gamma(0.1, 0.1) priors, for $a \in \{0, 1\}$. We assign Uniform(0, 0.5) priors to the spatial dependence parameters ρ . For each data set and scenario, MCMC is run for 120,000 iterations with the first 50,000 samples discarded as burn-in.

4.2 Results

We generate 200 data sets for each scenario. The causal estimand of interest is Δ given in (18). Table 1 reports bias, mean squared error (MSE) and 95% coverage probability (CP) for Δ . In comparing Scenarios 1 through 4, the discrepancy in model performance between the full and naive models becomes larger as the degree of preferential sampling increases (from $\phi = 0$ to

$\phi = 1$). Specifically, in Scenario 1 with no preferential sampling, both models show similar performance in terms of bias, MSE, and CP. With moderate preferential sampling in Scenario 2, the naive model exhibits poorer performance in terms of bias, MSE, and CP, while the full model shows almost similar performance compared to Scenario 1. In Scenarios 3 and 4 with strong and extreme preferential sampling, respectively, the full model outperforms the naive model in terms of bias, MSE, and CP. Specifically, the CPs of the naive models drop significantly, while both the biases and MSEs increase. In contrast, the values of the full model remain similar to those observed in Scenarios 1 through 3. This demonstrates the impact on the estimation of the causal effect when preferential sampling is not considered.

We see in Scenario 5 that greater spatial dependence tends to reduce MSE when compared to Scenario 3 for both models. The full model still shows better performance than the naive model in terms of bias, MSE, and CP. In Scenario 6 where the total sample size is twice as large on average, the bias and MSE decreased for both the full and naive models compared to Scenario 3. The full model continues to outperform the naive model across all three measures.

In Scenario 7, the full model outperforms the naive model in terms of bias, MSE, and CP, while the performance of the full model is similar to that in Scenario 3. In Scenario 8, the full model is shown to have similar performance to that under Scenario 3, exhibiting the robustness to the misspecification of the point process models. However, the naive model shows similar performance compared to scenario 3 in terms of MSE and CP. Importantly, Scenarios 7 and 8 illustrate that the proposed model is robust to some forms of model misspecification.

5 Analysis of Australian marine protected areas

5.1 Data description

Gill et al. (2017, 2024) compiled underwater visual census data from MPA and non-MPA sites worldwide to understand the effect of MPA management and other factors upon the conservation outcomes. For more information on data compilation and the original data sources, see Gill et al. (2024). In this analysis, we focus on fish survey sites in Australian waters, comparing the effective-

	ϕ	ρ	λ^*	G	S	Bias		MSE		Coverage	
						Naive	Full	Naive	Full	Naive	Full
1	0.0	0.1	5	✓	✓	-0.2 (0.3)	-0.5 (0.3)	0.2 (0.0)	0.2 (0.0)	95.0 (1.5)	96.5 (1.3)
2	1/3	0.1	5	✓	✓	6.8 (0.5)	-0.7 (0.6)	1.0 (0.1)	0.6 (0.1)	80.5 (2.8)	93.0 (1.8)
3	2/3	0.1	5	✓	✓	20.6 (0.8)	-1.7 (0.8)	5.6 (0.4)	1.2 (0.1)	48.0 (3.5)	97.5 (1.1)
4	1.0	0.1	5	✓	✓	40.3 (1.5)	-1.8 (1.5)	20.6 (1.5)	4.5 (0.7)	32.5 (3.3)	94.0 (1.7)
5	2/3	0.2	5	✓	✓	13.6 (0.7)	-0.3 (0.6)	2.8 (0.2)	0.8 (0.1)	69.0 (3.3)	96.5 (1.3)
6	2/3	0.1	10	✓	✓	17.5 (0.7)	-1.3 (0.6)	4.0 (0.3)	0.8 (0.1)	42.5 (3.5)	96.0 (1.4)
7	2/3	0.1	5	✓		22.1 (0.9)	0.4 (0.9)	6.4 (0.5)	1.7 (0.2)	49.5 (3.5)	95.5 (1.5)
8	2/3	0.1	5		✓	10.4 (0.8)	-4.3 (0.8)	2.5 (0.2)	1.6 (0.2)	80.5 (2.8)	93.5 (1.7)

Table 1: Bias, mean squared error (MSE) and coverage of 95% intervals for Δ are reported by comparing the full model to the naive model that ignores preferential sampling. The first six scenarios are defined by the strength of preferential sampling (ϕ), the strength of spatial dependence (ρ) and the intensity of sampling locations (λ^*). The final two scenarios generate data with non-Gaussian and non-stationary spatial processes. “G” stands for Gaussianity and “S” stands for stationarity. All values are multiplied by 100 and standard errors are given in parentheses.

ness of MPA policies with areas that have no protection. The observed outcome $Y(\mathbf{s})$ at a location $\mathbf{s} \in \mathcal{D}$ is the logarithm of fish biomass density ($\text{g}/100\text{m}^2$) defined in (Gill et al., 2017). Out of 3,553 survey sites, 2,609 received the marine protection policy ($A(\mathbf{s}) = 1$) and 944 did not ($A(\mathbf{s}) = 0$). Note that non-MPA sites within one kilometer of MPA boundaries were excluded from the original data to avoid a possible spillover effect (Gill et al., 2017, 2024). We use $p = 7$ covariates: distance to shoreline (km), depth (m), mean chlorophyll-a (year 2002 – 2009, mg/m^3), minimum sea surface temperature (year 2002 – 2009, $^\circ\text{C}$), human population density within a radius of 100 km from survey sites (year 2000, the number of individuals), distance to nearest markets (km) and habitat type (coral or rocky reefs). The spatial domain of interest is confined to the region within $0.5m_S$ from the shoreline or 150 km within the survey sites, covered by grid cells 0.8×0.8 degree², where $m_S \approx 265$ km is the maximum distance between the survey sites and the shoreline, approximately, and the number of grid cells is $G = 465$ cells (Figure 1). We also fit the model with coarser and finer values of grid cell resolutions and the results are similar (see D in Appendix). This domain is constrained to regions where environmental and social factors are similar to the survey sites. Covariates are obtained at the centroids of the grid cells and at the coordinates of the survey sites

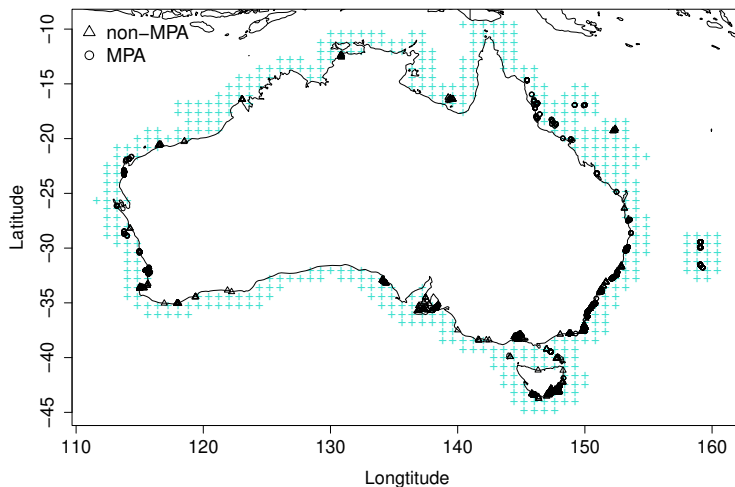


Figure 1: Domain of interest (Turquoise) and grid cell locations. Circular dots represent MPA sites, and triangular dots represent non-MPA sites.

by following or slightly modifying the procedure in Gill et al. (2017) (see E in Appendix). For the human population density, the values are log transformed after adding 1 to mitigate skewness. Missing values in the mean chlorophyll-a and the minimum sea surface temperature for the grid cells are imputed using the sample means of those with complete data, while missing values for the survey sites are imputed using the mean chlorophyll-a and the minimum sea surface temperature of the grid cells where the survey sites are located. The grid-level covariates and those measured at the survey sites are scaled to have mean zero and variance one collectively.

5.2 Model details

We consider both the “full” model in (12) – (17) and “naive” model, which assumes no preferential sampling with $\phi_0 = \phi_1 = 0$. Exploratory analysis suggested similar covariate effects across policies so we set $\beta_0 = \beta_1 = \beta$ and $\delta_0 = \delta_1 = \delta$. We assign the same prior distributions as those defined in Section 4.1 to most model parameters, except for the spatial dependence parameters, which we assign $\log(\rho_u)$ and $\log(\rho_v)$ each $\text{Normal}\{\log(300), 0.5\}$, and $\log(\kappa_u)$ and $\log(\kappa_v)$ each $\text{Normal}\{\log(0.5), 1\}$. MCMC is again used for model inference where the chains are run for 205,000 iterations and the first 5,000 are discarded as burn-in. The resulting chain is thinned to

	shoreline	depth	chlorophyll	temperature	population	distance	habitat
β	-0.08 (0.13)	9.25 (1.81)	0.06 (0.04)	1.01 (0.17)	-0.08 (0.24)	0.63 (0.27)	-0.76 (0.63)
δ	-0.95 (0.54)	-1.03 (0.29)	-0.44 (0.85)	-1.02 (1.07)	2.36 (0.67)	0.06 (0.73)	-0.56 (1.99)

Table 2: Posterior means (standard deviations) of the covariate effects on biomass (β) and sampling intensity (δ) for the full model applied to the Australia coast.

every 10th such that 20,000 posterior samples are retained for inference.

5.3 Results

We compare the full and naive models to investigate the impacts of preferential sampling on model inference, including estimating causal effects. Table 2 summarizes the posterior distributions of β and δ in the full model. The depth, minimum sea surface temperature, and distance to the markets have statistically significant effects. Fish biomass tends to increase as the survey site is deeper, which coincides with research that bathymetry and fish biomass are positively correlated (Boswell et al., 2010). More fish biomass is expected as the sea surface temperature increases. We conjecture that this is due to a negative correlation between sea surface temperature and habitat type. Coral reefs tend to be in the northern part of Australia, where sea temperature is relatively higher than in the southern part with more rocky reefs. We obtain a positive posterior mean estimate of the coefficient of distance to markets, which is natural since fish biomass is higher in regions with less human accessibility (Williams et al., 2008). The depth and the human population density have statistically significant effects on the sampling process. The negative coefficient estimate of depth and the positive coefficient estimate of human population density indicate that the survey tended to be focused on sites with greater accessibility.

Table 3 summarizes the posterior distributions of the parameters α_0 , α_1 , ϕ_0 , and ϕ_1 from the full model. Since the covariates are mean-centered, the posterior means of α_1 and α_0 can be interpreted as the average fish biomass with and without MPA policies respectively, when all other covariates are set to their mean values. The difference $\alpha_1 - \alpha_0$ can thus be interpreted as a global causal effect, which has a posterior mean 0.61 and standard deviation 0.74. This implies that the implementation of MPAs has a positive effect on the preservation of fish biodiversity, although it is not significant.

	α_0	α_1	ϕ_0	ϕ_1	γ_u	γ_v	r_u	r_v
Mean (SD)	7.24 (1.04)	7.85 (1.14)	0.61 (1.34)	-1.09 (2.17)	0.44 (0.33)	5.40 (6.22)	0.46 (0.32)	0.70 (0.47)

Table 3: Posterior means (standard deviations) of parameters for the full model

The positive posterior mean of ϕ_0 reported in Table 3 suggests non-MPA sites are sampled where fish biomass is high, while the negative mean of ϕ_1 indicates MPA sites are sampled where biomass is lower. We conjecture that the survey was conducted for MPA sites in favor of more accessible regions in which fish biomass is lower due to human access. Evidence can be found from the posterior mean values of δ in Table 2, suggesting that the surveys were carried out in regions closer to the shorelines, with shallower depth and with a larger human population. The posterior mean and the 95% credible interval of $\phi_1 - \phi_0$ are -1.70 and $(-5.67, 1.26)$. Since approximately 82% of the posterior mass of $\phi_1 - \phi_0$ is negative, we suggest that the degree of preferential sampling varies between the MPA and non-MPA sites.

Table 3 also summarizes the posterior distributions of the parameters γ_u , γ_v , r_u , and r_v from the full model, where r_u (and similarly r_v) is defined as the correlation coefficient between $U_{0,g}$ and $U_{1,g}$ for all g , computed as

$$r_u = \frac{\gamma_u \cdot \sigma_{u,0}^2}{\sqrt{\sigma_{u,0}^2(\sigma_{u,1}^2 + \gamma_u^2 \cdot \sigma_{u,0}^2)}}. \quad (23)$$

The positive posterior means of r_u and r_v suggest that the spatial processes $U_{0,g}$ and $U_{1,g}$ are positively correlated, and so are $V_{0,g}$ and $V_{1,g}$.

The marginal posterior distribution of Δ under both models is shown in Figure 2. The mean posteriors of Δ from the full and naive models are 0.71 and 0.27, respectively. Although both models estimate that implementing MPAs is superior to not doing so in terms of fish biodiversity on average, the naive model produces more conservative results compared to the full model. The 95% credible intervals being $(-0.24, 1.71)$ and $(-0.32, 0.87)$ under the full and naive models, respectively.

The upper left panel of Figure 3 presents the posterior means of the propensity score $\frac{\lambda_{1,g}}{\lambda_{0,g} + \lambda_{1,g}}$ at each grid cell. The propensity score estimate in the northern and southern parts of \mathcal{D} indicate

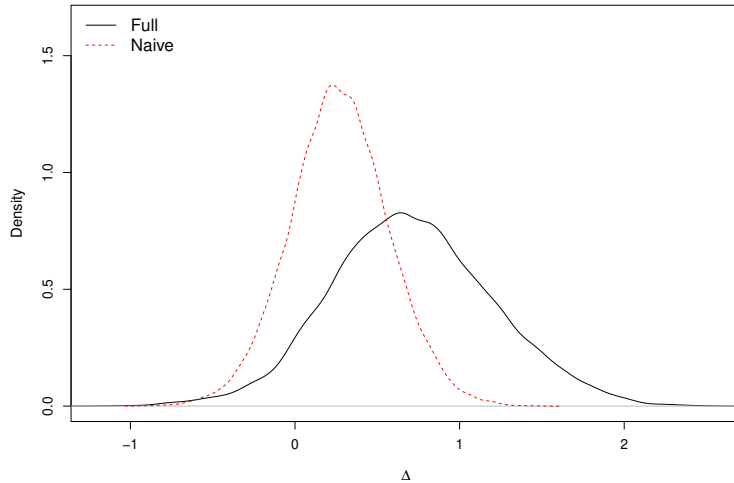


Figure 2: Posterior distributions of Δ (logarithm of $g/100m^2$) under the full and naive models.

that these regions are less likely to be assigned MPA policies, whereas the estimates in the eastern and western parts of \mathcal{D} are more likely to be assigned MPA policies. Specifically, the eastern and western regions of Australia align with the coral reef area (Figure 1 of Dixon et al., 2022), where their conservation is of great concern (Edgar et al., 2014). This is potential evidence that the MPA sites were sampled preferentially.

The upper right and lower left panels of Figure 3 show the posterior means and standard deviations, respectively, of the local causal effects $\alpha_1 - \alpha_0 + U_{1,g} - U_{0,g}$. Local causal effects are positive for the majority of the grid cells, implying that the implementation of MPAs is helpful in preserving fish biodiversity in these grid cells. The lower right panel of Figure 3 presents the difference between the posterior mean of the local causal effect under the full and naive model. As indicated in the figure provided, the naive model tends to give smaller estimates of the local causal effect across most grid cells.

6 Discussion

In this article, we present a novel approach to spatial causal inference that adjusts for bias introduced by preferential sampling. We model the response processes and point processes jointly

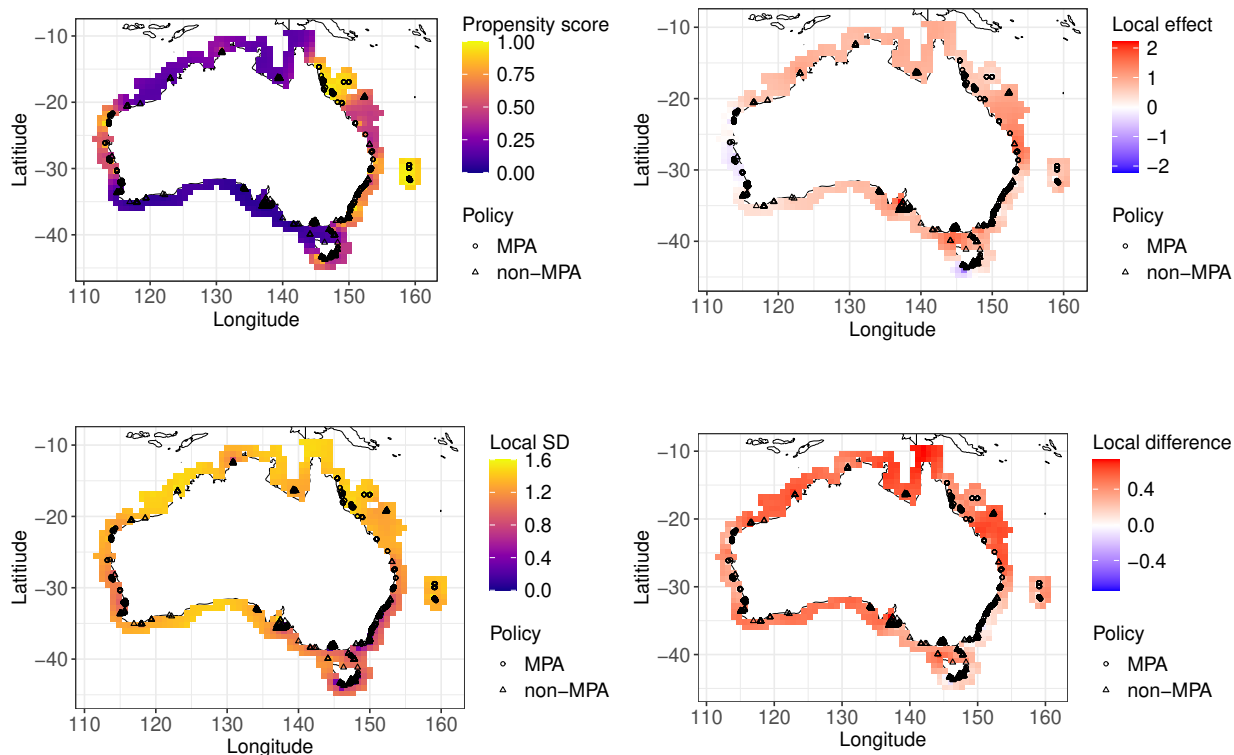


Figure 3: Posterior means of propensity scores $\frac{\lambda_{1,g}}{\lambda_{0,g} + \lambda_{1,g}}$ at each grid cell, along with the sampling locations (Upper left), posterior mean (Upper right) and standard deviation (Lower left) of local causal effects Δ_g under the full model, and the difference between posterior mean of local causal effects Δ_g under the full and naive model (Lower right)

using shared random effects to address preferential sampling. Our theoretical studies reveal that the parameters of interest are identifiable and the posterior distribution of the model parameters is weakly consistent. Our simulation study shows that the proposed model has valid coverage under the scenarios we considered, and that both bias and mean-squared error are reduced when compared to the naive model that does not account for preferential sampling. We apply the proposed method to study the impacts of MPA implementation on fish biomass on the Australian coast. We find evidence of preferential sampling and that consideration of the preferential sampling affects the causal effect.

To examine the plausibility of the SUTVA, latent ignorability, and positivity assumptions for the application to MPA data, we argue that the SUTVA assumption is justifiable since the non-

MPA sites within one kilometer of the MPA boundaries were removed from the data to prevent spatial interference (Gill et al., 2017, 2024). Although latent ignorability is typically not a testable assumption, similar to the unconfoundedness assumption in classical causal inference (Li et al., 2023), but we include many key covariates to support this assumption. Finally, we suggest that the positivity assumption is satisfied as the posterior means of the propensity scores are strictly between 0 and 1.

Some limitations of the proposed model exist that can be improved in future research. First, even if some non-MPA sites showing proximity to MPA regions were excluded from the data, there can be potential interference between MPA and non-MPA sites due to various attributes such as fish movement. Second, the proposed model specifies the mean of the response variables and the log intensities of the sampling process as linear models, which may be unrealistic. Third, the proposed model assumes that the propensity scores of all units in a grid cell are the same. However, since policies (treatments) are assigned to units rather than grid cells, future work is required for additional flexibility. Finally, sensitivity analysis is necessary to examine whether there exist unmeasured confounders, since social, political, and ecological factors determine MPA placement (Devillers et al., 2015), sampling of survey points, and fish biomass. Considering the aspects mentioned above for developing spatial causal inference methods taking the preferential sampling into account represents a promising direction for future research.

Acknowledgements

This work was supported in part by NSF grant DMS2152887, NIH grant R01ES031651-01, and USGS Climate Adaptation Science Center grant G22AC00597-01.

References

- Adler, R. J. and Taylor, J. E. (2009) *Random fields and geometry*. Springer Science & Business Media.
- Banerjee, S., Carlin, B. P. and Gelfand, A. E. (2003) *Hierarchical modeling and analysis for spatial data*. Chapman and Hall/CRC.
- Beaman, R. J. (2023) AusBathyTopo (Australia) 250m 2023 - A High-resolution Depth Model (20230004C). URL <https://doi.org/10.26186/148758>.
- Boswell, K. M., Wells, R., Cowan Jr, J. H. and Wilson, C. A. (2010) Biomass, density, and size distributions of fishes associated with a large-scale artificial reef complex in the Gulf of Mexico. *Bulletin of Marine Science*, **86**, 879–889.
- Campbell, S. J., Darling, E. S., Pardede, S., Ahmadia, G., Mangubhai, S., Amkieltiela, Estradivari and Maire, E. (2020) Fishing restrictions and remoteness deliver conservation outcomes for Indonesia's coral reef fisheries. *Conservation Letters*, **13**, e12698.
- Center for International Earth Science Information Network - CIESIN - Columbia University (2018) Gridded Population of the World, Version 4.11 (GPWv4): Population Count, Revision 11. URL <https://doi.org/10.7927/H4JW8BX5>. Accessed 15th August 2023.
- Cinner, J. E., Graham, N. A., Huchery, C. and MacNeil, M. A. (2013) Global effects of local human population density and distance to markets on the condition of coral reef fisheries. *Conservation Biology*, **27**, 453–458.
- Davis, M. L., Neelon, B., Nietert, P. J., Hunt, K. J., Burgette, L. F., Lawson, A. B. and Egede, L. E. (2019) Addressing geographic confounding through spatial propensity scores: a study of racial disparities in diabetes. *Statistical Methods in Medical Research*, **28**, 734–748.
- De Oliveira, V. and Han, Z. (2022) On information about covariance parameters in Gaussian Matérn random fields. *Journal of Agricultural, Biological and Environmental Statistics*, **27**, 690–712.
- Desbureaux, S., Girard, J., Dalongeville, A., Devillers, R., Mouillot, D., Jiddawi, N., Sanchez, L., Velez, L., Mathon, L. and Leblois, A. (2024) The long-term impacts of marine protected areas on fish catch and socioeconomic development in tanzania. *Conservation Letters*, e13048.
- Devillers, R., Pressey, R. L., Grech, A., Kittinger, J. N., Edgar, G. J., Ward, T. and Watson, R. (2015) Reinventing residual reserves in the sea: are we favouring ease of establishment over need for protection? *Aquatic conservation: marine and freshwater ecosystems*, **25**, 480–504.
- Diggle, P. J., Menezes, R. and Su, T.-I. (2010) Geostatistical inference under preferential sampling. *Journal of the Royal Statistical Society Series C: Applied Statistics*, **59**, 191–232.

- Ding, P. and Li, F. (2018) Causal inference: a missing data perspective. *Statistical Science*, **33**, 214–237.
- Dixon, A. M., Puotinen, M., Ramsay, H. A. and Beger, M. (2022) Coral reef exposure to damaging tropical cyclone waves in a warming climate. *Earth's Future*, **10**, e2021EF002600.
- Durrett, R. (1999) *Essentials of stochastic processes*, vol. 1. Springer.
- Edgar, G. J., Stuart-Smith, R. D., Willis, T. J., Kininmonth, S., Baker, S. C., Banks, S., Barrett, N. S., Becerro, M. A., Bernard, A. T., Berkhout, J. et al. (2014) Global conservation outcomes depend on marine protected areas with five key features. *Nature*, **506**, 216–220.
- ESRI (2023) World Cities. URL <https://www.arcgis.com/home/item.html?id=dfab3b294ab24961899b2a98e9e8cd3d>. Accessed: 6th September 2023.
- Ferraro, P. J., Sanchirico, J. N. and Smith, M. D. (2019) Causal inference in coupled human and natural systems. *Proceedings of the National Academy of Sciences*, **116**, 5311–5318.
- Gelfand, A. E., Sahu, S. K. and Holland, D. M. (2012) On the effect of preferential sampling in spatial prediction. *Environmetrics*, **23**, 565–578.
- Gelfand, A. E. and Schliep, E. M. (2018) Bayesian inference and computing for spatial point patterns. In *NSF-CBMS Regional Conference Series in Probability and Statistics*, vol. 10, i–125. JSTOR.
- Ghosal, S. and Roy, A. (2006) Posterior consistency of gaussian process prior for nonparametric binary regression. *The Annals of Statistics*.
- Ghosal, S. and Van der Vaart, A. (2017) *Fundamentals of nonparametric Bayesian inference*, vol. 44. Cambridge University Press.
- Ghosh, J. K. and Ramamoorthi, R. V. (2003) *Bayesian nonparametrics*. Springer series in statistics. New York: Springer-Verlag.
- Gill, D. A., Cheng, S. H., Glew, L., Aigner, E., Bennett, N. J. and Mascia, M. B. (2019) Social synergies, tradeoffs, and equity in marine conservation impacts. *Annual Review of Environment and Resources*, **44**, 347–372.
- Gill, D. A., Lester, S. E., Free, C. M., Pfaff, A., Iversen, E., Reich, B. J., Yang, S., Ahmadi, G., Andradi-Brown, D. A., Darling, E. S. et al. (2024) A diverse portfolio of marine protected areas can better advance global conservation and equity. *Proceedings of the National Academy of Sciences*, **121**, e2313205121.
- Gill, D. A., Mascia, M. B., Ahmadi, G. N., Glew, L., Lester, S. E., Barnes, M., Craigie, I., Darling, E. S., Free, C. M., Geldmann, J. et al. (2017) Capacity shortfalls hinder the performance of marine protected areas globally. *Nature*, **543**, 665–669.

- Gockenbach, M. S. (2011) *Finite-dimensional linear algebra*. CRC Press.
- Grorud-Colvert, K., Sullivan-Stack, J., Roberts, C., Constant, V., Horta e Costa, B., Pike, E. P., Kingston, N., Laffoley, D., Sala, E., Claudet, J. et al. (2021) The MPA guide: A framework to achieve global goals for the ocean. *Science*, **373**, eabf0861.
- Guan, Y., Page, G. L., Reich, B. J., Ventrucci, M. and Yang, S. (2023) Spectral adjustment for spatial confounding. *Biometrika*, **110**, 699–719.
- Hernán, M. A. and Robins, J. M. (2010) Causal inference.
- Imbens, G. W. and Rubin, D. B. (2015) *Causal inference in statistics, social, and biomedical sciences*. Cambridge University Press.
- IUCN, W. (2018) Applying IUCN’s Global Conservation Standards to Marine Protected Areas (MPAs). Delivering effective conservation action through MPAs, to secure ocean health & sustainable development. Version 1.0.
- Jarner, M. F., Diggle, P. and Chetwynd, A. G. (2002) Estimation of spatial variation in risk using matched case-control data. *Biometrical Journal: Journal of Mathematical Methods in Biosciences*, **44**, 936–945.
- Kamat, V. R. (2014) ” the ocean is our farm”: marine conservation, food insecurity, and social suffering in southeastern tanzania. *Human Organization*, **73**, 289–298.
- Knowles, J. E., Doyle, E., Schill, S. R., Roth, L. M., Milam, A. and Raber, G. T. (2015) Establishing a marine conservation baseline for the insular Caribbean. *Marine Policy*, **60**, 84–97.
- Laforgia, A. (1991) Bounds for modified bessel functions. *Journal of Computational and Applied Mathematics*, **34**, 263–267.
- Li, F., Ding, P. and Mealli, F. (2023) Bayesian causal inference: a critical review. *Philosophical Transactions of the Royal Society A*, **381**, 20220153.
- Marques, I., Kneib, T. and Klein, N. (2022) Mitigating spatial confounding by explicitly correlating Gaussian random fields. *Environmetrics*, **33**, e2727.
- Møller, J., Syversveen, A. R. and Waagepetersen, R. P. (1998) Log Gaussian Cox processes. *Scandinavian Journal of Statistics*, **25**, 451–482.
- Neal, R. M. et al. (2011) MCMC using Hamiltonian dynamics. *Handbook of Markov Chain Monte Carlo*, **2**, 2.
- Olver, F. W. (2010) *NIST handbook of mathematical functions*. Cambridge university press.
- Pati, D., Reich, B. J. and Dunson, D. B. (2011) Bayesian geostatistical modelling with informative sampling locations. *Biometrika*, **98**, 35–48.

- Reich, B. J., Yang, S., Guan, Y., Giffin, A. B., Miller, M. J. and Rappold, A. (2021) A review of spatial causal inference methods for environmental and epidemiological applications. *International Statistical Review*, **89**, 605–634.
- Rosenbaum, P. R. and Rubin, D. B. (1983) The central role of the propensity score in observational studies for causal effects. *Biometrika*, **70**, 41–55.
- Rubin, D. B. (1974) Estimating Causal effects of treatments in randomized and nonrandomized studies. *Journal of Educational Psychology*, **66**, 688.
- (1978) Bayesian inference for causal effects: The role of randomization. *The Annals of Statistics*, 34–58.
- Schliep, E. M., Wikle, C. K. and Daw, R. (2023) Correcting for informative sampling in spatial covariance estimation and kriging predictions. *Journal of Geographical Systems*, 1–27.
- Schnell, P. M. and Papadogeorgou, G. (2020) Mitigating unobserved spatial confounding when estimating the effect of supermarket access on cardiovascular disease deaths. *The Annals of Applied Statistics*, **14**, 2069 – 2095.
- Schwartz, L. (1965) On bayes procedures. *Zeitschrift für Wahrscheinlichkeitstheorie und verwandte Gebiete*, **4**, 10–26.
- Tyberghein, L., Verbruggen, H., Pauly, K., Troupin, C., Mineur, F. and De Clerck, O. (2012) Bio-ORACLE: a global environmental dataset for marine species distribution modelling. *Global Ecology and Biogeography*, **21**, 272–281.
- UNEP-WCMC, I. (2018) NGS.(2018). *Protected planet report*, **70**.
- Wessel, P. and Smith, W. H. (1996) A global, self-consistent, hierarchical, high-resolution shoreline database. *Journal of Geophysical Research: Solid Earth*, **101**, 8741–8743.
- Williams, C. K. and Rasmussen, C. E. (2006) *Gaussian processes for machine learning*, vol. 2. MIT press Cambridge, MA.
- Williams, I. D., Walsh, W., Schroeder, R., Friedlander, A., Richards, B. and Stamoulis, K. (2008) Assessing the importance of fishing impacts on Hawaiian coral reef fish assemblages along regional-scale human population gradients. *Environmental Conservation*, **35**, 261–272.

Appendix

A Details of the bias calculation

In this section we derive the approximate bias introduced to the causal effect by preferential sampling given in (9). We let observed covariates $\mathbf{X}(\mathbf{s})$ for $\mathbf{s} \in \mathcal{D}$ fixed. By the law of iterated expectations, we have

$$\mathbb{E}\{Y_1(\mathbf{s})\} = \mathbb{E}_{\mathcal{W}} \left[\mathbb{E}_{\mathcal{S}} \left\{ \alpha_1 + \mathbf{X}(\mathbf{s})^\top \boldsymbol{\beta}_1 + U_1(\mathbf{s}) \right\} \right]$$

where $\mathbb{E}_{\mathcal{W}}(\cdot)$ and $\mathbb{E}_{\mathcal{S}}(\cdot)$ are expectations with respect to spatial random effects and point processes respectively. Then,

$$\begin{aligned} & \mathbb{E}_{\mathcal{S}} \left\{ \alpha_1 + \mathbf{X}(\mathbf{s})^\top \boldsymbol{\beta}_1 + U_1(\mathbf{s}) \right\} \\ &= \alpha_1 + \frac{\int_{\mathcal{D}} \left\{ \mathbf{X}(\mathbf{w})^\top \boldsymbol{\beta}_1 + U_1(\mathbf{s}) \right\} \cdot \exp \left\{ \mathbf{X}(\mathbf{w})^\top \boldsymbol{\delta}_1 + V_1(\mathbf{w}) + \phi_1 U_1(\mathbf{w}) \right\} d\mathbf{w}}{\int_{\mathcal{D}} \exp \left\{ \mathbf{X}(\mathbf{w})^\top \boldsymbol{\delta}_1 + V_1(\mathbf{w}) + \phi_1 U_1(\mathbf{w}) \right\} d\mathbf{w}} \end{aligned}$$

since the location densities have form (6). Then $\mathbb{E}\{Y_1(\mathbf{s})\}$ is equivalent to

$$\alpha_1 + \mathbb{E}_{\mathcal{W}} \left[\frac{\int_{\mathcal{D}} \left\{ \mathbf{X}(\mathbf{w})^\top \boldsymbol{\beta}_1 + U_1(\mathbf{s}) \right\} \cdot \exp \left\{ \mathbf{X}(\mathbf{w})^\top \boldsymbol{\delta}_1 + V_1(\mathbf{w}) + \phi_1 U_1(\mathbf{w}) \right\} d\mathbf{w}}{\int_{\mathcal{D}} \exp \left\{ \mathbf{X}(\mathbf{w})^\top \boldsymbol{\delta}_1 + V_1(\mathbf{w}) + \phi_1 U_1(\mathbf{w}) \right\} d\mathbf{w}} \right].$$

Using the first-order Taylor expansion, the expectation of the ratio is approximated to the ratio of the expectations, i.e.,

$$\mathbb{E}\{Y_1(\mathbf{s})\} \approx \alpha_1 + \frac{\mathbb{E}_{\mathcal{W}} \left[\int_{\mathcal{D}} \left\{ \mathbf{X}(\mathbf{w})^\top \boldsymbol{\beta}_1 + U_1(\mathbf{s}) \right\} \cdot \exp \left\{ \mathbf{X}(\mathbf{w})^\top \boldsymbol{\delta}_1 + V_1(\mathbf{w}) + \phi_1 U_1(\mathbf{w}) \right\} d\mathbf{w} \right]}{\mathbb{E}_{\mathcal{W}} \left[\int_{\mathcal{D}} \exp \left\{ \mathbf{X}(\mathbf{w})^\top \boldsymbol{\delta}_1 + V_1(\mathbf{w}) + \phi_1 U_1(\mathbf{w}) \right\} d\mathbf{w} \right]}.$$

By Fubini's theorem, we can interchange the integral and the expectation in the denominator of the second term, i.e.,

$$\int_{\mathcal{D}} \mathbb{E}_{\mathcal{W}} \left[\exp \left\{ \mathbf{X}(\mathbf{w})^\top \boldsymbol{\delta}_1 + V_1(\mathbf{w}) + \phi_1 U_1(\mathbf{w}) \right\} \right] d\mathbf{w}.$$

Note that $\mathbf{X}(\mathbf{w})^\top \boldsymbol{\delta}_1 + V_1(\mathbf{w}) + \phi_1 U_1(\mathbf{w})$ follows a normal distribution with mean $\mathbf{X}(\mathbf{w})^\top \boldsymbol{\delta}_1$ and variance $\text{Var}(V_1) + \phi_1^2 \text{Var}(U_1)$. The variance does not depend on \mathbf{w} since we assume stationary processes. Accordingly, we have

$$\begin{aligned} & \int_{\mathcal{D}} \mathbb{E}_{\mathcal{W}} [\exp \{ \mathbf{X}(\mathbf{w})^\top \boldsymbol{\delta}_1 + V_1(\mathbf{w}) + \phi_1 U_1(\mathbf{w}) \}] d\mathbf{w} \\ &= \exp \left\{ \frac{\text{Var}(V_1) + \phi_1^2 \text{Var}(U_1)}{2} \right\} \int_{\mathcal{D}} \exp \{ \mathbf{X}(\mathbf{w})^\top \boldsymbol{\delta}_1 \} d\mathbf{w}. \end{aligned}$$

Using the law of iterated expectations, we also have

$$\begin{aligned} & \int_{\mathcal{D}} \mathbb{E}_{\mathcal{W}} [U_1(\mathbf{w}) \cdot \exp \{ \mathbf{X}(\mathbf{w})^\top \boldsymbol{\delta}_1 + V_1(\mathbf{w}) + \phi_1 U_1(\mathbf{w}) \}] d\mathbf{w} \\ &= \phi_1 \text{Var}(U_1) \cdot \exp \left\{ \frac{\text{Var}(V_1) + \phi_1^2 \text{Var}(U_1)}{2} \right\} \int_{\mathcal{D}} \exp \{ \mathbf{X}(\mathbf{w})^\top \boldsymbol{\delta}_1 \} d\mathbf{w}. \end{aligned}$$

Therefore, we have $\mathbb{E} \{ Y_1(\mathbf{s}) \} \approx \alpha_1 + \bar{\mathbf{X}}_1 \boldsymbol{\beta}_1 + \phi_1 \text{Var}(U_1)$. If we do the same steps for $\mathbb{E} \{ Y_0(\mathbf{s}) \}$, the expectation becomes (9).

B Proofs of Theorem 1 and Theorem 2

The proof of the Theorem 1

Our final model discretizes the spatial domain \mathcal{D} and assigns observations to G equally-sized grid cells $\{\mathcal{D}_1, \dots, \mathcal{D}_G\}$ with centroids $\{\mathbf{c}_1, \dots, \mathbf{c}_G\}$. Recall that $g(\mathbf{s}_i)$ be the index of the grid cell assigned to the observation at \mathbf{s}_i , i.e., $g(\mathbf{s}_i) = k$ if $\mathbf{s}_i \in \mathcal{D}_k$. The covariates and spatial processes at the centroids are denoted $\mathbf{X}(\mathbf{c}_k) = \mathbf{X}_k$, $U_a(\mathbf{c}_k) = U_{a,k}$ and $V_a(\mathbf{c}_k) = V_{a,k}$. The joint model for

$a \in \{0, 1\}$ is

$$\begin{aligned}
Y_a(\mathbf{s}_i) | \mathbf{s}_i, \mathbf{X}(\mathbf{s}_i), \boldsymbol{\theta}, \mathcal{W} &\stackrel{\text{indep}}{\sim} \text{Normal} \{ \alpha_a + \mathbf{X}(\mathbf{s}_i)^\top \boldsymbol{\beta}_a + U_{a,g(\mathbf{s}_i)}, \tau_a^2 \} \\
p_a(\mathbf{s}_i \in \mathcal{D}_k | \mathcal{X}, \boldsymbol{\theta}, \mathcal{W}) = \pi_{a,k} &= \frac{\exp \{ \mathbf{X}_k^\top \boldsymbol{\delta}_a + V_{a,k} + \phi_a U_{a,k} \}}{\sum_{g=1}^G \exp \{ \mathbf{X}_g^\top \boldsymbol{\delta}_a + V_{a,g} + \phi_a U_{a,g} \}} \\
(U_{a,1}, \dots, U_{a,G})^\top | \boldsymbol{\theta} &\sim \text{Normal} \{ \mathbf{0}_G, \mathbf{R}_{U_a}(\boldsymbol{\theta}_C) \} \\
(V_{a,1}, \dots, V_{a,G})^\top | \boldsymbol{\theta} &\sim \text{Normal} \{ \mathbf{0}_G, \mathbf{R}_{V_a}(\boldsymbol{\theta}_C) \}
\end{aligned}$$

where $\mathcal{W} = \left\{ \left(\tilde{U}_a(\mathbf{s}), \tilde{V}_a(\mathbf{s}) \right) : \mathbf{s} \in \mathcal{D}, a \in \{0, 1\} \right\}$, and the covariance matrices \mathbf{R}_{U_a} and \mathbf{R}_{V_a} are defined by the parameters $\boldsymbol{\theta}_C$.

To show identifiability using only the data requires marginalizing over the latent processes \mathcal{W} , which is immediate for the outcome variables but challenging for the Poisson process for the sampling locations. However, under the positivity assumption, for large n the proportion of the observations that fall in grid cell k will converge to $\pi_{ak} = \lambda_{a,k} / \sum_{g=1}^G \lambda_{a,g} > 0$. The set of π_{ak} is one-to-one with the set of linear predictors $L_{a,k} = \log(\lambda_{a,k}) = \eta_a + \mathbf{X}_k^\top \boldsymbol{\delta}_a + V_{a,k} + \phi_a U_{a,k}$ across the grid cells, which follows a multivariate normal distribution, facilitating marginalization over \mathcal{W} . Then the marginal distributions of $\mathbf{Y}_a = (Y_a(\mathbf{s}), \dots, Y_a(\mathbf{s}_n))^\top$ and $\mathbf{L}_a = (L_{a,1}, \dots, L_{a,G})^\top$ are

$$\begin{aligned}
\mathbf{Y}_a | \boldsymbol{\theta} &\sim \text{Normal} \{ \alpha_a \mathbf{1}_n + \mathbf{X}_S \boldsymbol{\beta}_a, \mathbf{H} \mathbf{R}_{U_a}(\boldsymbol{\theta}_C) \mathbf{H}^\top + \tau_a^2 \mathbb{I}_n \} \\
\mathbf{L}_a | \boldsymbol{\theta} &\sim \text{Normal} \{ \eta_a \mathbf{1}_G + \mathbf{X}_G \boldsymbol{\delta}_a, \mathbf{R}_{V_a}(\boldsymbol{\theta}_C) + \phi_a^2 \mathbf{R}_{U_a}(\boldsymbol{\theta}_C) \}
\end{aligned}$$

where \mathbf{X}_S , \mathbf{H} , and \mathbf{X}_G are the same as defined in Appendix A.

We say that $\boldsymbol{\theta}$ is identifiable if and only if $\ell(\mathbf{D} | \boldsymbol{\theta}^{(1)}) = \ell(\mathbf{D} | \boldsymbol{\theta}^{(2)})$ implies $\boldsymbol{\theta}^{(1)} = \boldsymbol{\theta}^{(2)}$ where $\ell(\cdot)$ is a generic notation for likelihood and $\mathbf{D} = (\mathbf{Y}_0, \mathbf{Y}_1, \mathbf{L}_0, \mathbf{L}_1)$. Since both \mathbf{Y}_a and \mathbf{L}_a are normally distributed, so is \mathbf{D} . Then, showing the identifiability is equivalent to proving that the mean vector and covariance matrix of \mathbf{D} parametrized by $\boldsymbol{\theta}$ is an one-to-one function of $\boldsymbol{\theta}$.

We start with the identification of ϕ_0 . Comparing \mathbf{s} and \mathbf{s}_i' in different grid cells immediately

identifies ϕ_0 since

$$\begin{aligned}\text{Cov} \{Y_0(\mathbf{s}_i), Y_0(\mathbf{s}_{i'})\} &= \sigma_{u,0}^2 \mathcal{R} (\|\mathbf{c}_{g(\mathbf{s}_i)} - \mathbf{c}_{g(\mathbf{s}_{i'})}\|; \kappa_u, \rho_u) \text{ and} \\ \text{Cov} \{Y_0(\mathbf{s}_i), L_{0,g(\mathbf{s}_{i'})}\} &= \phi_0 \sigma_{u,0}^2 \mathcal{R} (\|\mathbf{c}_{g(\mathbf{s}_i)} - \mathbf{c}_{g(\mathbf{s}_{i'})}\|; \kappa_u, \rho_u).\end{aligned}$$

Furthermore, since $\text{Cov} \{Y_0(\mathbf{s}_i), L_{0,g(\mathbf{s}_i)}\} = \phi_0 \sigma_{u,0}^2$ and since ϕ_0 has been identified, so has $\sigma_{u,0}^2$. To identify τ_0^2 , κ_u , and ρ_u , suppose $\text{Var} (\mathbf{Y}_0 | \boldsymbol{\theta}^{(1)}) = \text{Var} (\mathbf{Y}_0 | \boldsymbol{\theta}^{(2)})$. Comparing the diagonal elements is equivalent to $\sigma_{u,0}^2 + \left(\tau_0^{(1)}\right)^2 = \sigma_{u,0}^2 + \left(\tau_0^{(2)}\right)^2$, implying that $\left(\tau_0^{(1)}\right)^2 = \left(\tau_0^{(2)}\right)^2$. Thus, τ_0^2 is identified. Furthermore, comparing the off-diagonal elements is equivalent to

$$\sigma_{u,0}^2 \mathcal{R} (\|\mathbf{c}_{g(\mathbf{s}_i)} - \mathbf{c}_{g(\mathbf{s}_{i'})}\|; \kappa_u^{(1)}, \rho_u^{(1)}) = \sigma_{u,0}^2 \mathcal{R} (\|\mathbf{c}_{g(\mathbf{s}_i)} - \mathbf{c}_{g(\mathbf{s}_{i'})}\|; \kappa_u^{(2)}, \rho_u^{(2)})$$

for all $i, i' \in \{1, \dots, n\}$ since we have $\frac{n(n-1)}{2}$ equations for 2 variables. Therefore, κ_u and ρ_u are identified. See De Oliveira and Han (2022) for more details regarding estimation of the parameters of the Matérn covariance function. They suggested that geostatistical data contain as much information for the estimation of the smoothness parameter of a Matérn kernel as the range parameter, which is opposed to the tradition that rather fixes the smoothness parameter.

For the identification of γ_u , observe that $\text{Cov} \{Y_0(\mathbf{s}_i), Y_1(\mathbf{s}_i)\} = \gamma_u \sigma_{u,0}^2$. Since $\sigma_{u,0}^2$ has been identified, γ_u is also identified. Now suppose $\text{Var} (\mathbf{Y}_1 | \boldsymbol{\theta}^{(1)}) = \text{Var} (\mathbf{Y}_1 | \boldsymbol{\theta}^{(2)})$. By comparing the off-diagonal elements, we have

$$\left\{ \left(\sigma_{u,1}^{(1)}\right)^2 + \gamma_u^2 \sigma_{u,0}^2 \right\} \mathcal{R} (\|\mathbf{c}_{g(\mathbf{s}_i)} - \mathbf{c}_{g(\mathbf{s}_{i'})}\|; \kappa_u, \rho_u) = \left\{ \left(\sigma_{u,1}^{(2)}\right)^2 + \gamma_u^2 \sigma_{u,0}^2 \right\} \mathcal{R} (\|\mathbf{c}_{g(\mathbf{s}_i)} - \mathbf{c}_{g(\mathbf{s}_{i'})}\|; \kappa_u, \rho_u)$$

implying that $\left\{ \sigma_{u,1}^{(1)} \right\}^2 = \left\{ \sigma_{u,1}^{(2)} \right\}^2$. Therefore, $\sigma_{u,1}^2$ is identified. Then, by comparing the diagonal elements from $\text{Var} (\mathbf{Y}_1 | \boldsymbol{\theta}^{(1)}) = \text{Var} (\mathbf{Y}_1 | \boldsymbol{\theta}^{(2)})$, we can identify τ_1^2 . Since $\text{Var}(L_{0,g}) = \sigma_{v,0}^2 + \phi_0^2 \sigma_{u,0}^2$, comparing the diagonal elements of $\text{Var} (\mathbf{L}_0 | \boldsymbol{\theta}^{(1)}) = \text{Var} (\mathbf{L}_0 | \boldsymbol{\theta}^{(2)})$ immediately identifies $\sigma_{v,0}^2$. Similarly as above, comparing the off-diagonal elements yields

$$\sigma_{v,0}^2 \mathcal{R} (\|\mathbf{c}_g - \mathbf{c}_{g'}\|; \kappa_v^{(1)}, \rho_v^{(1)}) = \sigma_{v,0}^2 \mathcal{R} (\|\mathbf{c}_g - \mathbf{c}_{g'}\|; \kappa_v^{(2)}, \rho_v^{(2)})$$

for all $g, g' \in \{1, \dots, G\}$, implying that κ_v and ρ_v are identified.

To identify ϕ_1 , consider

$$\text{Cov} \{Y_1(\mathbf{s}_i), L_{1,g(\mathbf{s}_i)}\} = \text{Cov} \{U_{1,g(\mathbf{s}_i)}, \phi_1 U_{1,g(\mathbf{s}_i)}\} = \phi_1 (\sigma_{u,1}^2 + \gamma_u \sigma_{u,0}^2).$$

Since $\sigma_{u,0}^2$, $\sigma_{u,1}^2$, and γ_u have been identified, the identification of ϕ_1 is immediate. For identifying γ_v , consider $\text{Cov}(L_{0,g}, L_{1,g}) = \gamma_v \sigma_{v,0}^2 + \gamma_u \phi_0 \phi_1 \sigma_{u,0}^2$. This quantity identifies γ_v since $\sigma_{v,0}^2$, γ_u , ϕ_0 , ϕ_1 , and $\sigma_{u,0}^2$ have been identified. Since $\text{Var}(L_{1,g}) = \sigma_{v,1}^2 + \gamma_v^2 \sigma_{v,0}^2 + \phi_1^2 (\sigma_{u,1}^2 + \gamma_u \sigma_{u,0}^2)$, $\sigma_{v,1}^2$ is identified as all the other parameters involving $\text{Var}(L_{1,g})$ have been identified. Finally, the identification of α_a , β_a , η_a and δ_a is guaranteed by Assumption 5. This ends the proof of the identifiability of θ .

The proof of the Theorem 2

Let $\omega = (\theta_{\mathcal{M}}, \mathcal{W})$ be the parameters in the causal effect Δ . Denote an arbitrary observation as $\mathbf{Z} = (Y, A, \mathbf{s})$ and note that the observations $(\mathbf{Z}_1, \dots, \mathbf{Z}_n)$ are independently and identically distributed conditioned on ω . Denote the joint density of \mathbf{Z} given a set of covariates \mathcal{X} and parameters ω as $f(\mathbf{Z}|\omega)$ and the prior of ω as $\Pi(\omega)$, where the vector of hyperparameters $\theta_{\mathcal{C}}$ is assigned by the priors that satisfies Assumption 4. To prove weak consistency of a posterior distribution of ω , we define a Kullback-Leibler (K-L) support (Ghosal and Van der Vaart, 2017; Ghosh and Ramamoorthi, 2003) to utilize a result from Schwartz (1965) that if Definition 1 is satisfied, then the posterior of ω is weakly consistent (Ghosh and Ramamoorthi, 2003).

Definition 1. *The density f at the true value ω^* is said to be in the K-L support of the prior Π if*

$$\Pi \{ \omega : K(\omega^*, \omega) < \varepsilon \} > 0$$

for all $\varepsilon > 0$, where $K(\omega^*, \omega) = \int \log \frac{f(\mathbf{Z}|\omega^*)}{f(\mathbf{Z}|\omega)} f(\mathbf{Z}|\omega^*) d\mathbf{z}$ is a Kullback-Leibler (K-L) divergence.

To show that $f(\mathbf{Z}|\boldsymbol{\omega}^*)$ is in the K-L support of the prior Π , we define a ν -ball $B_\nu(\boldsymbol{\omega}^*)$ to be

$$\cap_{a=0}^1 \left\{ \boldsymbol{\omega} : |\alpha_a - \alpha_a^*| < \nu, \|\boldsymbol{\beta}_a - \boldsymbol{\beta}_a^*\|_2 < \nu, |\eta_a - \eta_a^*| < \nu, \|\boldsymbol{\delta}_a - \boldsymbol{\delta}_a^*\|_2 < \nu, |\phi_a - \phi_a^*| < \nu, \right. \\ \left. |\tau_a/\tau_a^* - 1| < \nu, \|\tilde{U}_a - \tilde{U}_a^*\|_\infty < \nu, \|\tilde{V}_a - \tilde{V}_a^*\|_\infty < \nu, |\gamma_u - \gamma_u^*| < \nu, |\gamma_v - \gamma_v^*| < \nu \right\}$$

for some $\nu > 0$. The proof proceeds by first showing that for every $\varepsilon > 0$ there exists a $\nu > 0$ such that for all $\boldsymbol{\omega} \in B_\nu(\boldsymbol{\omega}^*)$ we have $K(\boldsymbol{\omega}, \boldsymbol{\omega}^*) < \varepsilon$. We then show that the prior probability on $\{\boldsymbol{\omega} : \boldsymbol{\omega} \in B_\nu(\boldsymbol{\omega}^*)\}$ is positive to complete the proof.

Under Assumption 1 and Assumption 2, the joint density can be decomposed as

$$f(\mathbf{Z}|\boldsymbol{\omega}) = f_a(Y_a|\mathbf{s}, \boldsymbol{\omega})p_a(\mathbf{s}|\boldsymbol{\omega})\mathbb{P}(A = a|\boldsymbol{\omega})$$

where $f_a(Y_a|\mathbf{s}, \boldsymbol{\omega})$ is the density of the potential outcome given \mathbf{s} and $\boldsymbol{\omega}$, $p_a(\mathbf{s}|\boldsymbol{\omega})$ is the location density for \mathcal{S}_a given $\boldsymbol{\omega}$, and

$$\mathbb{P}(A = a|\boldsymbol{\omega}) = \frac{\int_{\mathcal{D}} \lambda_a(\mathbf{s})d\mathbf{s}}{\int_{\mathcal{D}} \lambda_0(\mathbf{s})d\mathbf{s} + \int_{\mathcal{D}} \lambda_1(\mathbf{s})d\mathbf{s}}$$

for $a \in \{0, 1\}$.

The KL divergence is decomposed into two parts as

$$K(\boldsymbol{\omega}^*, \boldsymbol{\omega}) = K_1(\boldsymbol{\omega}^*, \boldsymbol{\omega})\mathbb{P}(A = 1|\boldsymbol{\omega}^*) + K_0(\boldsymbol{\omega}^*, \boldsymbol{\omega})\mathbb{P}(A = 0|\boldsymbol{\omega}^*) < K_1(\boldsymbol{\omega}^*, \boldsymbol{\omega}) + K_0(\boldsymbol{\omega}^*, \boldsymbol{\omega})$$

where

$$K_a(\boldsymbol{\omega}^*, \boldsymbol{\omega}) = \int \log \frac{f_a(Y_a|\mathbf{s}, \boldsymbol{\omega}^*)p_a(\mathbf{s}|\boldsymbol{\omega}^*)\mathbb{P}(A = a|\boldsymbol{\omega}^*)}{f_a(Y_a|\mathbf{s}, \boldsymbol{\omega})p_a(\mathbf{s}|\boldsymbol{\omega})\mathbb{P}(A = a|\boldsymbol{\omega})} f_a(Y_a|\mathbf{s}, \boldsymbol{\omega})p_a(\mathbf{s}|\boldsymbol{\omega})dY_a d\mathbf{s}.$$

We focus on $K_1(\boldsymbol{\omega}^*, \boldsymbol{\omega})$, and a similar argument can be applied to $K_0(\boldsymbol{\omega}^*, \boldsymbol{\omega})$. The steps given below are based on the proof of the Theorem 1 in Pati et al. (2011). Let $\mu_1(\mathbf{s}) = \alpha_1 + \mathbf{X}(\mathbf{s})^\top \boldsymbol{\beta}_1 + U_1(\mathbf{s})$, $U_1(\mathbf{s}) = \tilde{U}_1(\mathbf{s}) + \gamma_u \tilde{U}_0(\mathbf{s})$ and $V_1(\mathbf{s}) = \tilde{V}_1(\mathbf{s}) + \gamma_v \tilde{V}_0(\mathbf{s})$, while $\mu_1^*(\mathbf{s})$, $U_1^*(\mathbf{s})$, and $V_1^*(\mathbf{s})$ are

those evaluated at $\boldsymbol{\omega}^*$. Then,

$$K_1(\boldsymbol{\omega}^*, \boldsymbol{\omega}) = \frac{1}{2} \log \frac{\tau_1^2}{(\tau_1^*)^2} - \frac{1}{2} \left\{ 1 - \frac{(\tau_1^*)^2}{\tau_1^2} \right\} + \frac{1}{2\tau_1^2} \int_{\mathcal{D}} \{\mu_1^*(\mathbf{s}) - \mu_1(\mathbf{s})\}^2 p_1(\mathbf{s}|\boldsymbol{\omega}^*) d\mathbf{s} \quad (\text{A1})$$

$$- \int_{\mathcal{D}} \{ \mathbf{X}(\mathbf{s})^\top (\boldsymbol{\delta}_1 - \boldsymbol{\delta}_1^*) + V_1(\mathbf{s}) - V_1^*(\mathbf{s}) + \phi_1 U_1(\mathbf{s}) - \phi_1^* U_1^*(\mathbf{s}) \} p_1(\mathbf{s}|\boldsymbol{\omega}) d\mathbf{s} \quad (\text{A2})$$

$$+ \log \left[\frac{\int_{\mathcal{D}} \exp \{ \mathbf{X}(\mathbf{s})^\top \boldsymbol{\delta}_1 + V_1(\mathbf{s}) + \phi_1 U_1(\mathbf{s}) \} d\mathbf{s}}{\int_{\mathcal{D}} \exp \{ \mathbf{X}(\mathbf{s})^\top \boldsymbol{\delta}_1^* + V_1^*(\mathbf{s}) + \phi_1^* U_1^*(\mathbf{s}) \} d\mathbf{s}} \right] \quad (\text{A3})$$

$$+ \log \frac{\mathbb{P}(A = 1|\boldsymbol{\omega}^*)}{\mathbb{P}(A = 1|\boldsymbol{\omega})}. \quad (\text{A4})$$

Let the ℓ_∞ -norm for a bounded function $h \in \mathcal{C}(\mathcal{D})$ as $\|h\|_\infty = \sup_{\mathbf{s} \in \mathcal{D}} |h(\mathbf{s})|$ and denote the ℓ_2 norm of a vector \mathbf{v} as $\|\mathbf{v}\|_2$. For (A1), we clearly have

$$\begin{aligned} \frac{1}{2} \log \frac{\tau_1^2}{(\tau_1^*)^2} - \frac{1}{2} \left(1 - \frac{(\tau_1^*)^2}{\tau_1^2} \right) + \frac{1}{2\tau_1^2} \int_{\mathcal{D}} \{\mu_1^*(\mathbf{s}) - \mu_1(\mathbf{s})\}^2 p_1(\mathbf{s}|\boldsymbol{\omega}^*) d\mathbf{s} \\ \leq \frac{1}{2} \log \frac{\tau_1^2}{(\tau_1^*)^2} - \frac{1}{2} \left(1 - \frac{(\tau_1^*)^2}{\tau_1^2} \right) + \frac{\|\mu_1^* - \mu_1\|_\infty^2}{2\tau_1^2}. \end{aligned} \quad (\text{A5})$$

By using the equivalence of a norm (Gockenbach, 2011), there exists $\tilde{C}_1 > 0$ such that $\|\boldsymbol{\beta}_1^* - \boldsymbol{\beta}_1\|_\infty \leq \tilde{C}_1 \|\boldsymbol{\beta}_1^* - \boldsymbol{\beta}_1\|_2$. Using the assumption that $\|\mathbf{X}(\mathbf{s})\| \leq C$ for all $\mathbf{s} \in \mathcal{D}$, Cauchy-Schwarz inequality, and triangle inequality, we have the following.

$$\|\mu_1^* - \mu_1\|_\infty = \|\alpha_1 - \alpha_1^* + \mathbf{X}^\top (\boldsymbol{\beta}_1 - \boldsymbol{\beta}_1^*) + U_1 - U_1^*\|_\infty \leq |\alpha_1 - \alpha_1^*| + C_1 \|\boldsymbol{\beta}_1 - \boldsymbol{\beta}_1^*\|_2 + \|U_1 - U_1^*\|_\infty$$

where $C_1 = C \cdot \tilde{C}_1$. By the LMC and triangle inequality,

$$\|U_1 - U_1^*\|_\infty \leq \|\tilde{U}_1 - \tilde{U}_1^*\|_\infty + \|\gamma_u \tilde{U}_0 - \gamma_u^* \tilde{U}_0^*\|_\infty.$$

Therefore, since all the terms in the right hand side of (A5) are bounded, for all $\varepsilon > 0$, there exists $\nu_1 > 0$ such that $\boldsymbol{\omega} \in B_{\nu_1}$ implies

$$\frac{1}{2} \log \frac{\tau_1^2}{(\tau_1^*)^2} - \frac{1}{2} \left(1 - \frac{(\tau_1^*)^2}{\tau_1^2} \right) + \frac{1}{2\tau_1^2} \int_{\mathcal{D}} \{\mu_1^*(\mathbf{s}) - \mu_1(\mathbf{s})\}^2 p_1(\mathbf{s}|\boldsymbol{\omega}^*) d\mathbf{s} < \varepsilon/8.$$

Second, let us proceed to (A2). Due to the norm equivalence, Cauchy-Schwarz inequality, and triangle inequality, we have

$$\begin{aligned}
& \mathbf{X}(\mathbf{s})^\top (\boldsymbol{\delta}_1 - \boldsymbol{\delta}_1^*) + V_1(\mathbf{s}) - V_1^*(\mathbf{s}) + \phi_1 U_1(\mathbf{s}) - \phi_1^* U_1^*(\mathbf{s}) \\
& \leq |\mathbf{X}(\mathbf{s})^\top (\boldsymbol{\delta}_1 - \boldsymbol{\delta}_1^*) + V_1(\mathbf{s}) - V_1^*(\mathbf{s}) + \phi_1 U_1(\mathbf{s}) - \phi_1^* U_1^*(\mathbf{s})| \\
& \leq \tilde{C}_2 \|\boldsymbol{\delta}_1 - \boldsymbol{\delta}_1^*\|_2 + \|V_1 - V_1^*\|_\infty + \|\phi_1 U_1 - \phi_1^* U_1^*\|_\infty.
\end{aligned}$$

By the LMC, we have $\|V_1 - V_{1,*}\|_\infty \leq \|\tilde{V}_1 - \tilde{V}_1^*\|_\infty + \|\gamma_v \tilde{V}_0 - \gamma_v^* \tilde{V}_0^*\|_\infty$. By the LMC and triangle inequality,

$$\|\phi_1 U_1 - \phi_{1,*} U_{1,*}\|_\infty \leq \|\phi_1 \tilde{U}_1 - \phi_1^* \tilde{U}_1^*\|_\infty + \|\phi_1 \gamma_u \tilde{U}_0 - \phi_1^* \gamma_u^* \tilde{U}_0^*\|_\infty.$$

Then, there exists $\nu_2 > 0$ such that for $\boldsymbol{\omega} \in B_{\nu_2}$,

$$\int_{\mathcal{D}} \{\mathbf{X}(\mathbf{s})^\top (\boldsymbol{\delta}_1 - \boldsymbol{\delta}_1^*) + V_1(\mathbf{s}) - V_1^*(\mathbf{s}) + \phi_1 U_1(\mathbf{s}) - \phi_1^* U_1^*(\mathbf{s})\} p_1(\mathbf{s}|\boldsymbol{\omega}) ds < \varepsilon/8.$$

For (A3), let

$$\Lambda_a(\boldsymbol{\omega}) = \log \left[\int_{\mathcal{D}} \exp \{ \mathbf{X}(\mathbf{s})^\top \boldsymbol{\delta}_a + V_a(\mathbf{s}) + \phi_a U_a(\mathbf{s}) \} ds \right].$$

Since $\exp \{ \mathbf{X}(\mathbf{s})^\top \boldsymbol{\delta}_a + V_a(\mathbf{s}) + \phi_a U_a(\mathbf{s}) \}$ is a continuous function in $\boldsymbol{\omega}$, so is Λ_a . By using this continuity, we can say that for all $\varepsilon > 0$, there exists $\nu_3 > 0$ such that $\boldsymbol{\omega} \in B_{\nu_3}$ implies

$$\log \left[\frac{\int_{\mathcal{D}} \exp \{ \mathbf{X}(\mathbf{s})^\top \boldsymbol{\delta}_1 + V_1(\mathbf{s}) + \phi_1 U_1(\mathbf{s}) \} ds}{\int_{\mathcal{D}} \exp \{ \mathbf{X}(\mathbf{s})^\top \boldsymbol{\delta}_1^* + V_1^*(\mathbf{s}) + \phi_1^* U_1^*(\mathbf{s}) \} ds} \right] < \varepsilon/8.$$

In a similar sense, for (A4), since $\lambda_0(\mathbf{s})$ and $\lambda_1(\mathbf{s})$ are continuous functions in $\boldsymbol{\omega}$ and so is $\mathbb{P}(A = 1|\boldsymbol{\omega})$. Therefore, for all $\varepsilon > 0$, there exists $\nu_4 > 0$ such that $\boldsymbol{\omega} \in B_{\nu_4}$ implies

$$\log \frac{\mathbb{P}(A = 1|\boldsymbol{\omega}^*)}{\mathbb{P}(A = 1|\boldsymbol{\omega})} < \varepsilon/8.$$

Finally, by taking $\nu = \min \{\nu_1, \nu_2, \nu_3, \nu_4\}$, $\omega \in B_\nu$ implies

$$K_1(\omega^*, \omega) < \varepsilon/2.$$

It can be verified that this result holds for $K_0(\omega^*, \omega)$ by following similar steps and we have $K(\omega^*, \omega) < \varepsilon$.

To complete the proof, we show that the prior probability on $\{\omega : \omega \in B_\nu(\omega^*)\}$ is positive. If we assign priors to $\theta_{\mathcal{M}}$ as described in Assumption 4, the prior distribution of $\theta_{\mathcal{M}}$ has a positive probability for $\omega \in B_\nu(\omega^*)$. For the prior positivity of \mathcal{W} , we require the following lemma.

Lemma 1. *Let $U(\mathbf{s})$ be a mean-zero Gaussian process on $\mathcal{D} \subseteq \mathbb{R}^2$ with a Matérn covariance kernel parametrized by variance σ^2 , spatial dependence ρ , and smoothness parameter κ . Then, $U(\mathbf{s})$ has a continuous sample path if $\kappa \geq 1/2$.*

Proof. The proof uses a result from Adler and Taylor (2009) that requires a bound on

$$\mathbb{E} \{|U(\mathbf{s}) - U(\mathbf{s}')|^2\} = 2\sigma^2 \{1 - \mathcal{R}(h; \rho, \kappa)\},$$

where $h = \|\mathbf{s} - \mathbf{s}'\|$ and $\mathcal{R}(h; \rho, \kappa)$ has the form (8). Since $\frac{\partial h^\kappa \mathcal{K}_\kappa(h)}{\partial h} = -h^\kappa \mathcal{K}_{\kappa-1}(h)$ (10.29.2 of Olver, 2010),

$$\left| \frac{\partial \mathcal{R}(h; \rho, \kappa)}{\partial h} \right| = M_1 \cdot \left(\frac{h}{\rho}\right)^\kappa \mathcal{K}_{\kappa-1}\left(\frac{h}{\rho}\right)$$

for some constant $M_1 > 0$. Since $\mathcal{K}_{\kappa-1}(h) < \mathcal{K}_\kappa(h)$ when $\kappa > 1/2$ (3.3 of Laforgia, 1991),

$$\left| \frac{\partial \mathcal{R}(h; \rho, \kappa)}{\partial h} \right| < M_1 \cdot \left(\frac{h}{\rho}\right)^\kappa \mathcal{K}_\kappa\left(\frac{h}{\rho}\right) = M_2 \cdot \mathcal{R}(h; \rho, \kappa) \leq M_2$$

for some constant $M_2 > 0$. When $\kappa = 1/2$, $\frac{\partial \mathcal{R}(h; \rho, \kappa)}{\partial h} \propto \exp(-h/\rho)$, which is bounded for all $h > 0$. Therefore, $\frac{\partial \mathcal{R}(h; \rho, \kappa)}{\partial h}$ is finite for $h > 0$ when $\kappa \geq 1/2$.

Let $C_{\text{sup}} = \sup_{h>0, \kappa \geq 1/2} \left| \frac{\partial \mathcal{R}(h; \rho, \kappa)}{\partial h} \right|$. By the mean value theorem and the boundedness of the

derivative of $\mathcal{R}(h; \rho, \kappa)$, we have

$$\mathbb{E} \{|U(\mathbf{s}) - U(\mathbf{s}')|^2\} = -\frac{\partial \mathcal{R}(h; \rho, \kappa)}{\partial h} \Big|_{h=h_0} \cdot 2\sigma^2 h \leq 2\sigma^2 C_{\text{sup}} \cdot h,$$

where h_0 lies in between 0 and h . Since $h \leq |\log(h)|^{-2}$ for $h < 1$,

$$\mathbb{E} \{|U(\mathbf{s}) - U(\mathbf{s}')|^2\} \leq \frac{2\sigma^2 C_{\text{sup}}}{|\log(h)|^2}$$

and by Theorem 1.4.1 from Adler and Taylor (2009), $U(\mathbf{s})$ has a continuous sample path. \square

We establish prior positivity for \mathcal{W} using Lemma 1 by conditioning on the events $\{\kappa_u \geq 1/2\}$ and $\{\kappa_v \geq 1/2\}$ following Theorem 4 of Ghosal and Roy (2006), which assumes the continuity of the sample paths of Gaussian processes. However, by Assumption 4 that we assign the smoothness parameters with the priors having positive mass on those events, the prior positivity of \mathcal{W} holds marginally over θ_C and subsequently

$$\Pi \{\boldsymbol{\omega} : \boldsymbol{\omega} \in B_\nu(\boldsymbol{\omega}^*)\} > 0.$$

Since $\boldsymbol{\omega} \in B_\nu$ implies $K(\boldsymbol{\omega}^*, \boldsymbol{\omega}) < \varepsilon$ for all $\varepsilon > 0$, we have

$$\Pi \{\boldsymbol{\omega} : K(\boldsymbol{\omega}^*, \boldsymbol{\omega}) < \varepsilon\} > 0.$$

Therefore, by Schwartz (1965), the posterior is weakly consistent and this completes the proof of Theorem 2.

C Derivations of the Gibbs sampler

Let us denote $q(\cdot|\cdot)$ a full conditional density, $\mathcal{L}(\cdot|\cdot)$ a likelihood, and $\pi(\cdot)$ a marginal prior density. Let us denote $\cdot|\text{rest}$ a full conditional distribution of a parameter conditioned on the remaining parameters.

Full conditional distribution for β_0, β_1

Let the prior be $\beta_a \sim \text{MVN}(\mathbf{0}_p, c_\beta^2 \mathbf{I}_p)$ for $a \in \{0, 1\}$. Let \mathbf{Y}_a be a $n \times 1$ vector of potential outcomes $Y_a(s_i)$ for $i = 1, \dots, n$ and \mathbf{X}_S be a $n \times p$ covariate matrix with i^{th} row corresponding to $\mathbf{X}(s_i)$, respectively. Note that \mathbf{Y}_a has complete entries since the missing values are imputed at every step of MCMC iterations. Let \mathbf{H} be a $n \times G$ matrix where (i, g) entry corresponds to 1 if i^{th} observation belongs to \mathcal{D}_g for some $g = 1, \dots, G$, and 0 otherwise. Then,

$$\begin{aligned}
& q(\beta_a | \text{rest}) \\
& \propto \mathcal{L}(\mathbf{Y}_a | \beta_a, \text{rest}) \pi(\beta_a) \\
& \propto \exp \left\{ -\frac{(\mathbf{Y}_a - \mathbf{H}\mathbf{U}_a - \alpha_a \mathbf{1}_n - \mathbf{X}_S \beta_a)^\top (\mathbf{Y}_a - \mathbf{H}\mathbf{U}_a - \alpha_a \mathbf{1}_n - \mathbf{X}_S \beta_a)}{2\tau_a^2} \right\} \times \\
& \quad \exp \left(-\frac{\beta_a^\top \beta_a}{2c_\beta^2} \right) \\
& \propto \exp \left\{ -\frac{\beta_a^\top \mathbf{X}_S^\top \mathbf{X}_S \beta_a - 2\beta_a^\top \mathbf{X}_S^\top (\mathbf{Y}_a - \mathbf{H}\mathbf{U}_a - \alpha_a \mathbf{1}_n)}{2\tau_a^2} \right\} \exp \left(-\frac{\beta_a^\top \beta_a}{2c_\beta^2} \right) \\
& \propto \exp \left[-\frac{1}{2} \left\{ \beta_a^\top \left(\frac{\mathbf{X}_S^\top \mathbf{X}_S}{\tau_a^2} + \frac{\mathbb{I}_p}{c_\beta^2} \right) \beta_a - \frac{2\beta_a^\top \mathbf{X}_S^\top (\mathbf{Y}_a - \mathbf{H}\mathbf{U}_a - \alpha_a \mathbf{1}_n)}{\tau_a^2} \right\} \right].
\end{aligned}$$

Thus,

$$\beta_a | \text{rest} \sim \text{MVN}(\mathbf{C}_a^{-1} \mathbf{b}_a, \mathbf{C}_a^{-1})$$

where $\mathbf{b}_a = \mathbf{X}_S^\top (\mathbf{Y}_a - \mathbf{H}\mathbf{U}_a - \alpha_a \mathbf{1}_n) / \tau_a^2$ and $\mathbf{C}_a = \mathbf{X}_S^\top \mathbf{X}_S / \tau_a^2 + \mathbb{I}_p / c_\beta^2$.

Full conditional distribution for α_0, α_1

Let the prior be $\alpha_a \sim \text{Normal}(0, c_\alpha^2)$ for $a \in \{0, 1\}$. Then,

$$\begin{aligned}
& q(\alpha_a | \text{rest}) \\
& \propto \mathcal{L}(\mathbf{Y}_a | \alpha_a, \text{rest}) \pi(\alpha_a) \\
& \propto \exp \left\{ -\frac{(\mathbf{Y}_a - \mathbf{H}\mathbf{U}_a - \alpha_a \mathbf{1}_n - \mathbf{X}_S \beta_a)^\top (\mathbf{Y}_a - \mathbf{H}\mathbf{U}_a - \alpha_a \mathbf{1}_n - \mathbf{X}_S \beta_a)}{2\tau_a^2} \right\} \exp \left(-\frac{\alpha_a^2}{2c_\alpha^2} \right) \\
& \propto \exp \left\{ -\frac{n \cdot \alpha_a^2 - 2\alpha_a \cdot \mathbf{1}_n^\top (\mathbf{Y}_a - \mathbf{H}\mathbf{U}_a - \mathbf{X}_S \beta_a)}{2\tau_a^2} \right\} \exp \left(-\frac{\alpha_a^2}{2c_\alpha^2} \right) \\
& \propto \exp \left[-\frac{1}{2} \left\{ \left(\frac{n}{\tau_a^2} + \frac{1}{c_\alpha^2} \right) \alpha_a^2 - \frac{2 \cdot \mathbf{1}_n^\top (\mathbf{Y}_a - \mathbf{H}\mathbf{U}_a - \mathbf{X}_S \beta_a)}{\tau_a^2} \alpha_a \right\} \right].
\end{aligned}$$

Thus,

$$\alpha_a | \text{rest} \sim \text{Normal}(b_a / C_a, 1 / C_a)$$

where $b_a = \mathbf{1}_n^\top (\mathbf{Y}_a - \mathbf{H}\mathbf{U}_a - \mathbf{X}_S \boldsymbol{\beta}_a) / \tau_a^2$ and $C_a = \left(\frac{n}{\tau_a^2} + \frac{1}{c_a^2} \right)$.

Full conditional distribution for δ_0, δ_1

Let the prior be $\boldsymbol{\delta}_a \sim \text{MVN}(\mathbf{0}_p, c_\delta^2 \mathbf{I}_p)$. Let \mathbf{L}_a be a $G \times 1$ vector with its g^{th} entry being $\log(\lambda_{a,g})$ and \mathbf{X}_G be a $G \times p$ matrix with every g^{th} row corresponding to \mathbf{X}_g . Then,

$$\begin{aligned} q(\boldsymbol{\delta}_a | \text{rest}) &\propto \mathcal{L}(\mathbf{L}_a | \boldsymbol{\delta}_a, \text{rest}) \pi(\boldsymbol{\delta}_a) \\ &\propto \exp \left\{ - \frac{(\mathbf{L}_a - \eta_a \mathbf{1}_G - \mathbf{X}_G \boldsymbol{\delta}_a - \mathbf{V}_a - \phi_a \mathbf{U}_a)^\top (\mathbf{L}_a - \eta_a \mathbf{1}_G - \mathbf{X}_G \boldsymbol{\delta}_a - \mathbf{V}_a - \phi_a \mathbf{U}_a)}{2\tau_{\psi_a}^2} \right\} \times \\ &\quad \exp \left(- \frac{\boldsymbol{\delta}_a^\top \boldsymbol{\delta}_a}{2c_\delta^2} \right) \\ &\propto \exp \left\{ - \frac{\boldsymbol{\delta}_a^\top \mathbf{X}_G^\top \mathbf{X}_G \boldsymbol{\delta}_a - 2\boldsymbol{\delta}_a^\top \mathbf{X}_G^\top (\mathbf{L}_a - \eta_a \mathbf{1}_G - \mathbf{V}_a - \phi_a \mathbf{U}_a)}{2\tau_{\psi_a}^2} \right\} \exp \left(- \frac{\boldsymbol{\delta}_a^\top \boldsymbol{\delta}_a}{2c_\delta^2} \right) \\ &\propto \exp \left[- \frac{1}{2} \left\{ \boldsymbol{\delta}_a^\top \left(\frac{\mathbf{X}_G^\top \mathbf{X}_G}{\tau_{\psi_a}^2} + \frac{\mathbb{I}_p}{c_\delta^2} \right) \boldsymbol{\delta}_a - \frac{2\boldsymbol{\delta}_a^\top \mathbf{X}_G^\top (\mathbf{L}_a - \eta_a \mathbf{1}_G - \mathbf{V}_a - \phi_a \mathbf{U}_a)}{\tau_{\psi_a}^2} \right\} \right]. \end{aligned}$$

Thus,

$$\boldsymbol{\delta}_a | \text{rest} \sim \text{MVN}(\mathbf{C}_a^{-1} \mathbf{b}_a, \mathbf{C}_a^{-1})$$

where $\mathbf{b}_a = \mathbf{X}_G^\top (\mathbf{L}_a - \eta_a \mathbf{1}_G - \mathbf{V}_a - \phi_a \mathbf{U}_a) / \tau_{\psi_a}^2$ and $\mathbf{C}_a = \mathbf{X}_G^\top \mathbf{X}_G / \tau_{\psi_a}^2 + \mathbb{I}_p / c_\delta^2$.

Full conditional distribution for η_0, η_1

Let the prior be $\eta_a \sim \text{Normal}(0, c_\eta^2)$. Then,

$$\begin{aligned}
& q(\eta_a | \text{rest}) \\
& \propto \mathcal{L}(\mathbf{L}_a | \eta_a, \text{rest}) \pi(\eta_a) \\
& \propto \exp \left\{ -\frac{(\mathbf{L}_a - \eta_a \mathbf{1}_G - \mathbf{X}_G \boldsymbol{\delta}_a - \mathbf{V}_a - \phi_a \mathbf{U}_a)^\top (\mathbf{L}_a - \eta_a \mathbf{1}_G - \mathbf{X}_G \boldsymbol{\delta}_a - \mathbf{V}_a - \phi_a \mathbf{U}_a)}{2\tau_{\psi_a}^2} \right\} \times \\
& \quad \exp \left(-\frac{\eta_a^2}{2c_\eta^2} \right) \\
& \propto \exp \left\{ -\frac{G \cdot \eta_a^2 - 2 \cdot \mathbf{1}_G^\top (\mathbf{L}_a - \mathbf{X}_G \boldsymbol{\delta}_a - \mathbf{V}_a - \phi_a \mathbf{U}_a)}{2\tau_{\psi_a}^2} \right\} \exp \left(-\frac{\eta_a^2}{2c_\eta^2} \right) \\
& \propto \exp \left[-\frac{1}{2} \left\{ \left(\frac{G}{\tau_{\psi_a}^2} + \frac{1}{c_\eta^2} \right) \eta_a^2 - \frac{2 \cdot \mathbf{1}_G^\top (\mathbf{L}_a - \mathbf{X}_G \boldsymbol{\delta}_a - \mathbf{V}_a - \phi_a \mathbf{U}_a)}{\tau_{\psi_a}^2} \eta_a \right\} \right].
\end{aligned}$$

Thus,

$$\eta_a | \text{rest} \sim \text{Normal}(b_a / C_a, 1 / C_a)$$

where $b_a = \mathbf{1}_G^\top (\mathbf{L}_a - \mathbf{X}_G \boldsymbol{\delta}_a - \mathbf{V}_a - \phi_a \mathbf{U}_a) / \tau_{\psi_a}^2$ and $C_a = \left(\frac{G}{\tau_{\psi_a}^2} + \frac{1}{c_\eta^2} \right)$.

Full conditional distribution for ϕ_0, ϕ_1

Let the prior be $\phi_a \sim \text{Normal}(0, c_\phi^2)$. Then,

$$\begin{aligned}
& q(\phi_a | \text{rest}) \\
& \propto \mathcal{L}(\mathbf{L}_a | \phi_a, \text{rest}) \pi(\phi_a) \\
& \propto \exp \left\{ -\frac{(\mathbf{L}_a - \eta_a \mathbf{1}_G - \mathbf{X}_G \boldsymbol{\delta}_a - \mathbf{V}_a - \phi_a \mathbf{U}_a)^\top (\mathbf{L}_a - \eta_a \mathbf{1}_G - \mathbf{X}_G \boldsymbol{\delta}_a - \mathbf{V}_a - \phi_a \mathbf{U}_a)}{2\tau_{\psi_a}^2} \right\} \times \\
& \quad \exp \left(-\frac{\phi_a^2}{2c_\phi^2} \right) \\
& \propto \exp \left\{ -\frac{\mathbf{U}_a^\top \mathbf{U}_a \phi_a^2 - 2\phi_a \cdot \mathbf{U}_a^\top (\mathbf{L}_a - \eta_a \mathbf{1}_G - \mathbf{X}_G \boldsymbol{\delta}_a - \mathbf{V}_a)}{2\tau_{\psi_a}^2} \right\} \exp \left(-\frac{\phi_a^2}{2c_\phi^2} \right) \\
& \propto \exp \left[-\frac{1}{2} \left\{ \left(\frac{\mathbf{U}_a^\top \mathbf{U}_a}{\tau_{\psi_a}^2} + \frac{1}{c_\phi^2} \right) \phi_a^2 - \frac{2 \cdot \mathbf{U}_a^\top (\mathbf{L}_a - \eta_a \mathbf{1}_G - \mathbf{X}_G \boldsymbol{\delta}_a - \mathbf{V}_a)}{\tau_{\psi_a}^2} \phi_a \right\} \right].
\end{aligned}$$

Thus,

$$\phi_a | \text{rest} \sim \text{Normal}(b_a / C_a, 1 / C_a)$$

where $b_a = \mathbf{U}_a^\top (\mathbf{L}_a - \eta_a \mathbf{1}_G - \mathbf{X}_G \boldsymbol{\delta}_a - \mathbf{V}_a) / \tau_{\psi_a}^2$ and $C_a = \left(\frac{\mathbf{U}_a^\top \mathbf{U}_a}{\tau_{\psi_a}^2} + \frac{1}{c_\eta^2} \right)$.

Full conditional distribution for γ_u

Let the prior be $\gamma_u \sim \text{Normal}(0, c_\gamma^2)$. By LMC, $\mathbf{U}_0 = \tilde{\mathbf{U}}_0$ and $\mathbf{U}_1 = \tilde{\mathbf{U}}_1 + \gamma_u \tilde{\mathbf{U}}_0$. Let $\mathbf{m}_{\beta_1} = \alpha_1 \mathbf{1}_n + \mathbf{X}_S \boldsymbol{\beta}_1$ and $\mathbf{m}_{\delta_1} = \eta_1 \mathbf{1}_G + \mathbf{X}_G \boldsymbol{\delta}_1$ for brevity of notation. Then,

$$\begin{aligned}
& q(\gamma_u | \text{rest}) \\
& \propto \mathcal{L}(\mathbf{Y}_1 | \gamma_u, \text{rest}) f(\mathbf{L}_1 | \gamma_u, \text{rest}) \pi(\gamma_u) \\
& \propto \exp \left\{ - \frac{(\mathbf{Y}_1 - \mathbf{m}_{\beta_1} - \mathbf{H}\tilde{\mathbf{U}}_1 - \gamma_u \cdot \mathbf{H}\tilde{\mathbf{U}}_0)^\top (\mathbf{Y}_1 - \mathbf{m}_{\beta_1} - \mathbf{H}\tilde{\mathbf{U}}_1 - \gamma_u \cdot \mathbf{H}\tilde{\mathbf{U}}_0)}{2\tau_1^2} \right\} \times \\
& \quad \exp \left\{ - \frac{(\mathbf{L}_1 - \mathbf{m}_{\delta_1} - \mathbf{V}_1 - \phi_1 \tilde{\mathbf{U}}_1 - \gamma_u \cdot \phi_1 \tilde{\mathbf{U}}_0)^\top (\mathbf{L}_1 - \mathbf{m}_{\delta_1} - \mathbf{V}_1 - \phi_1 \tilde{\mathbf{U}}_1 - \gamma_u \cdot \phi_1 \tilde{\mathbf{U}}_0)}{2\tau_{\psi_1}^2} \right\} \times \\
& \quad \exp \left(- \frac{\gamma_u^2}{2c_\gamma^2} \right) \\
& \propto \exp \left\{ - \frac{\tilde{\mathbf{U}}_0^\top \mathbf{H}^\top \mathbf{H} \tilde{\mathbf{U}}_0 \cdot \gamma_u^2 - 2\gamma_u \cdot \tilde{\mathbf{U}}_0^\top \mathbf{H}^\top (\mathbf{Y}_1 - \mathbf{m}_{\beta_1} - \mathbf{H}\tilde{\mathbf{U}}_1)}{2\tau_1^2} \right\} \times \\
& \quad \exp \left\{ - \frac{\phi_1^2 \tilde{\mathbf{U}}_0^\top \tilde{\mathbf{U}}_0 \cdot \gamma_u^2 - 2\gamma_u \cdot \phi_1 \tilde{\mathbf{U}}_0^\top (\mathbf{L}_1 - \mathbf{m}_{\delta_1} - \mathbf{V}_1 - \phi_1 \tilde{\mathbf{U}}_1)}{2\tau_{\psi_1}^2} \right\} \times \exp \left(- \frac{\gamma_u^2}{2c_\gamma^2} \right) \\
& \propto \exp \left\{ - \frac{1}{2} \left(\frac{\tilde{\mathbf{U}}_0^\top \mathbf{H}^\top \mathbf{H} \tilde{\mathbf{U}}_0}{\tau_1^2} + \frac{\phi_1^2 \tilde{\mathbf{U}}_0^\top \tilde{\mathbf{U}}_0}{\tau_{\psi_1}^2} + \frac{1}{c_\gamma^2} \right) \gamma_u^2 \right\} \times \\
& \quad \exp \left[- \left\{ \frac{\tilde{\mathbf{U}}_0^\top \mathbf{H}^\top (\mathbf{Y}_1 - \mathbf{m}_{\beta_1} - \mathbf{H}\tilde{\mathbf{U}}_1)}{\tau_1^2} + \frac{\phi_1 \tilde{\mathbf{U}}_0^\top (\mathbf{L}_1 - \mathbf{m}_{\delta_1} - \mathbf{V}_1 - \phi_1 \tilde{\mathbf{U}}_1)}{\tau_{\psi_1}^2} \right\} \gamma_u \right].
\end{aligned}$$

Thus,

$$\gamma_u | \text{rest} \sim \text{Normal}(b/C, 1/C)$$

where

$$b = \tilde{\mathbf{U}}_0^\top \mathbf{H}^\top (\mathbf{Y}_1 - \mathbf{m}_{\beta_1} - \mathbf{H}\tilde{\mathbf{U}}_1) / \tau_1^2 + \phi_1 \tilde{\mathbf{U}}_0^\top (\mathbf{L}_1 - \mathbf{m}_{\delta_1} - \mathbf{V}_1 - \phi_1 \tilde{\mathbf{U}}_1) / \tau_{\psi_1}^2$$

and

$$C = \left(\frac{\tilde{\mathbf{U}}_0^\top \mathbf{H}^\top \mathbf{H} \tilde{\mathbf{U}}_0}{\tau_1^2} + \frac{\phi_1^2 \tilde{\mathbf{U}}_0^\top \tilde{\mathbf{U}}_0}{\tau_{\psi_1}^2} + \frac{1}{c_\gamma^2} \right).$$

Full conditional distribution for γ_v

Let the prior be $\gamma_v \sim \text{Normal}(0, c_\gamma^2)$. By LMC, $\mathbf{V}_0 = \tilde{\mathbf{V}}_0$ and $\mathbf{V}_1 = \tilde{\mathbf{V}}_1 + \gamma_v \tilde{\mathbf{V}}_0$. Then,

$$\begin{aligned}
& q(\gamma_v | \text{rest}) \\
& \propto \mathcal{L}(\mathbf{L}_1 | \gamma_v, \text{rest}) \pi(\gamma_v) \\
& \propto \exp \left\{ -\frac{(\mathbf{L}_1 - \mathbf{m}_{\delta_1} - \tilde{\mathbf{V}}_1 - \gamma_v \tilde{\mathbf{V}}_0 - \phi_1 \mathbf{U}_1)^\top (\mathbf{L}_1 - \mathbf{m}_{\delta_1} - \tilde{\mathbf{V}}_1 - \gamma_v \tilde{\mathbf{V}}_0 - \phi_1 \mathbf{U}_1)}{2\tau_{\psi_1}^2} \right\} \times \\
& \quad \exp \left(-\frac{\gamma_v^2}{2c_\gamma^2} \right) \\
& \propto \exp \left\{ -\frac{\tilde{\mathbf{V}}_0^\top \tilde{\mathbf{V}}_0 \cdot \gamma_v^2 - 2\gamma_v \cdot \tilde{\mathbf{V}}_0^\top (\mathbf{L}_1 - \mathbf{m}_{\delta_1} - \tilde{\mathbf{V}}_1 - \phi_1 \mathbf{U}_1)}{2\tau_{\psi_1}^2} \right\} \times \exp \left(-\frac{\gamma_v^2}{2c_\gamma^2} \right) \\
& \propto \exp \left[-\frac{1}{2} \left\{ \left(\frac{\tilde{\mathbf{V}}_0^\top \tilde{\mathbf{V}}_0}{\tau_{\psi_1}^2} + \frac{1}{c_\gamma^2} \right) \gamma_v^2 + \frac{2\tilde{\mathbf{V}}_0^\top (\mathbf{L}_1 - \mathbf{m}_{\delta_1} - \tilde{\mathbf{V}}_1 - \phi_1 \mathbf{U}_1)}{\tau_{\psi_1}^2} \gamma_v \right\} \right].
\end{aligned}$$

Thus,

$$\gamma_u | \text{rest} \sim \text{Normal}(b/C, 1/C)$$

where $b = \tilde{\mathbf{V}}_0^\top (\mathbf{L}_1 - \mathbf{m}_{\delta_1} - \tilde{\mathbf{V}}_1 - \phi_1 \mathbf{U}_1) / \tau_{\psi_1}^2$ and $C = \left(\frac{\tilde{\mathbf{V}}_0^\top \tilde{\mathbf{V}}_0}{\tau_{\psi_1}^2} + \frac{1}{c_\gamma^2} \right)$.

Full conditional distribution for $\tilde{\mathbf{U}}_0$

Note that $\tilde{\mathbf{U}}_0 \sim \text{MVN}\{\mathbf{0}_G, \sigma_{u,0}^2 \mathbf{R}(\rho_u, \kappa_u)\}$. Let $\mathbf{m}_{\beta_0} = \alpha_0 \mathbf{1}_n + \mathbf{X}_S \boldsymbol{\beta}_0$ and $\mathbf{m}_{\delta_0} = \eta_0 \mathbf{1}_G + \mathbf{X}_G \boldsymbol{\delta}_0$ for

brevity. Then,

$$\begin{aligned}
& q(\tilde{\mathbf{U}}_0|\text{rest}) \\
& \propto \mathcal{L}(\mathbf{Y}_0|\tilde{\mathbf{U}}_0, \text{rest}) \mathcal{L}(\mathbf{Y}_1|\tilde{\mathbf{U}}_0, \text{rest}) \mathcal{L}(\mathbf{L}_0|\tilde{\mathbf{U}}_0, \text{rest}) \mathcal{L}(\mathbf{L}_1|\tilde{\mathbf{U}}_0, \text{rest}) \pi(\tilde{\mathbf{U}}_0) \\
& \propto \exp \left\{ -\frac{(\mathbf{Y}_0 - \mathbf{m}_{\beta_0} - \mathbf{H}\tilde{\mathbf{U}}_0)^\top (\mathbf{Y}_0 - \mathbf{m}_{\beta_0} - \mathbf{H}\tilde{\mathbf{U}}_0)}{2\tau_0^2} \right\} \times \\
& \quad \exp \left\{ -\frac{(\mathbf{Y}_1 - \mathbf{m}_{\beta_1} - \mathbf{H}\tilde{\mathbf{U}}_1 - \gamma_u \mathbf{H}\tilde{\mathbf{U}}_0)^\top (\mathbf{Y}_1 - \mathbf{m}_{\beta_1} - \mathbf{H}\tilde{\mathbf{U}}_1 - \gamma_u \mathbf{H}\tilde{\mathbf{U}}_0)}{2\tau_1^2} \right\} \times \\
& \quad \exp \left\{ -\frac{(\mathbf{L}_0 - \mathbf{m}_{\delta_0} - \mathbf{V}_0 - \phi_0 \tilde{\mathbf{U}}_0)^\top (\mathbf{L}_0 - \mathbf{m}_{\delta_0} - \mathbf{V}_0 - \phi_0 \tilde{\mathbf{U}}_0)}{2\tau_{\psi_0}^2} \right\} \times \\
& \quad \exp \left\{ -\frac{(\mathbf{L}_1 - \mathbf{m}_{\delta_1} - \mathbf{V}_1 - \phi_1 \tilde{\mathbf{U}}_1 - \phi_1 \gamma_u \tilde{\mathbf{U}}_0)^\top (\mathbf{L}_1 - \mathbf{m}_{\delta_1} - \mathbf{V}_1 - \phi_1 \tilde{\mathbf{U}}_1 - \phi_1 \gamma_u \tilde{\mathbf{U}}_0)}{2\tau_{\psi_1}^2} \right\} \times \\
& \quad \exp \left\{ -\frac{\tilde{\mathbf{U}}_0^\top \mathbf{R}^{-1}(\rho_u, \kappa_u) \tilde{\mathbf{U}}_0}{2\sigma_{u,0}^2} \right\} \\
& \propto \exp \left\{ -\frac{\tilde{\mathbf{U}}_0^\top \mathbf{H}^\top \mathbf{H} \tilde{\mathbf{U}}_0 - 2\tilde{\mathbf{U}}_0^\top \mathbf{H}^\top (\mathbf{Y}_0 - \mathbf{m}_{\beta_0})}{2\tau_0^2} \right\} \times \\
& \quad \exp \left\{ -\frac{\gamma_u^2 \tilde{\mathbf{U}}_0^\top \mathbf{H}^\top \mathbf{H} \tilde{\mathbf{U}}_0 - 2\gamma_u \tilde{\mathbf{U}}_0^\top \mathbf{H}^\top (\mathbf{Y}_1 - \mathbf{m}_{\beta_1} - \mathbf{H}\tilde{\mathbf{U}}_1)}{2\tau_1^2} \right\} \times \\
& \quad \exp \left\{ -\frac{\phi_0^2 \tilde{\mathbf{U}}_0^\top \tilde{\mathbf{U}}_0 - 2\phi_0 \tilde{\mathbf{U}}_0^\top (\mathbf{L}_0 - \mathbf{m}_{\delta_0} - \mathbf{V}_0)}{2\tau_{\psi_0}^2} \right\} \times \\
& \quad \exp \left\{ -\frac{(\phi_1 \gamma_u)^2 \tilde{\mathbf{U}}_0^\top \tilde{\mathbf{U}}_0 - 2\phi_1 \gamma_u \tilde{\mathbf{U}}_0^\top (\mathbf{L}_1 - \mathbf{m}_{\delta_1} - \mathbf{V}_1 - \phi_1 \tilde{\mathbf{U}}_1)}{2\tau_{\psi_1}^2} \right\} \exp \left\{ -\frac{\tilde{\mathbf{U}}_0^\top \mathbf{R}^{-1}(\rho_u, \kappa_u) \tilde{\mathbf{U}}_0}{2\sigma_{u,0}^2} \right\} \\
& \propto \exp \left[-\frac{1}{2} \left\{ \tilde{\mathbf{U}}_0^\top \left(\frac{\mathbf{H}^\top \mathbf{H}}{\tau_0^2} + \frac{\gamma_u^2 \mathbf{H}^\top \mathbf{H}}{\tau_1^2} + \frac{\phi_0^2 \mathbb{I}_G}{\tau_{\psi_0}^2} + \frac{\phi_1^2 \gamma_u^2 \mathbb{I}_G}{\tau_{\psi_1}^2} + \frac{\mathbf{R}^{-1}(\rho_u, \kappa_u)}{\sigma_{u,0}^2} \right) \tilde{\mathbf{U}}_0 \right\} \right] \times \\
& \quad \exp \left[-\tilde{\mathbf{U}}_0^\top \left\{ \frac{\mathbf{H}^\top (\mathbf{Y}_0 - \mathbf{m}_{\beta_0})}{\tau_0^2} + \frac{\gamma_u \mathbf{H}^\top (\mathbf{Y}_1 - \mathbf{m}_{\beta_1} - \mathbf{H}\tilde{\mathbf{U}}_1)}{\tau_1^2} + \frac{\phi_0 (\mathbf{L}_0 - \mathbf{m}_{\delta_0} - \mathbf{V}_0)}{\tau_{\psi_0}^2} \right\} \right] \times \\
& \quad \exp \left[-\tilde{\mathbf{U}}_0^\top \left\{ \frac{\phi_1 \gamma_u (\mathbf{L}_1 - \mathbf{m}_{\delta_1} - \mathbf{V}_1 - \phi_1 \tilde{\mathbf{U}}_1)}{\tau_{\psi_1}^2} \right\} \right].
\end{aligned}$$

Thus, $\tilde{\mathbf{U}}_0|\text{rest} \sim \text{MVN}(\mathbf{C}^{-1}\mathbf{b}, \mathbf{C}^{-1})$ where

$$\mathbf{b} = \frac{\mathbf{H}^\top (\mathbf{Y}_0 - \mathbf{m}_{\beta_0})}{\tau_0^2} + \frac{\gamma_u \mathbf{H}^\top (\mathbf{Y}_1 - \mathbf{m}_{\beta_1} - \mathbf{H}\tilde{\mathbf{U}}_1)}{\tau_1^2} + \frac{\phi_0 (\mathbf{L}_0 - \mathbf{m}_{\delta_0} - \mathbf{V}_0)}{\tau_{\psi_0}^2} + \frac{\phi_1 \gamma_u (\mathbf{L}_1 - \mathbf{m}_{\delta_1} - \mathbf{V}_1 - \phi_1 \tilde{\mathbf{U}}_1)}{\tau_{\psi_1}^2}$$

and

$$\mathbf{C} = \frac{\mathbf{H}^\top \mathbf{H}}{\tau_0^2} + \frac{\gamma_u^2 \mathbf{H}^\top \mathbf{H}}{\tau_1^2} + \frac{\phi_0^2 \mathbb{I}_G}{\tau_{\psi_0}^2} + \frac{\phi_1^2 \gamma_u^2 \mathbb{I}_G}{\tau_{\psi_1}^2} + \frac{\mathbf{R}^{-1}(\rho_u, \kappa_u)}{\sigma_{u,0}^2}.$$

Full conditional distribution for $\tilde{\mathbf{U}}_1$

Note that $\tilde{\mathbf{U}}_1 \sim \text{MVN}\{\mathbf{0}_G, \sigma_{u,1}^2 \mathbf{R}(\rho_u, \kappa_u)\}$. Then,

$$\begin{aligned} & q(\tilde{\mathbf{U}}_0 | \text{rest}) \\ & \propto \mathcal{L}(\mathbf{Y}_1 | \tilde{\mathbf{U}}_1, \text{rest}) \mathcal{L}(\mathbf{L}_1 | \tilde{\mathbf{U}}_1, \text{rest}) \pi(\tilde{\mathbf{U}}_1) \\ & \propto \exp \left\{ -\frac{(\mathbf{Y}_1 - \mathbf{m}_{\beta_1} - \mathbf{H}\tilde{\mathbf{U}}_1 - \gamma_u \mathbf{H}\tilde{\mathbf{U}}_0)^\top (\mathbf{Y}_1 - \mathbf{m}_{\beta_1} - \mathbf{H}\tilde{\mathbf{U}}_1 - \gamma_u \mathbf{H}\tilde{\mathbf{U}}_0)}{2\tau_1^2} \right\} \times \\ & \quad \exp \left\{ -\frac{(\mathbf{L}_1 - \mathbf{m}_{\delta_1} - \mathbf{V}_1 - \phi_1 \tilde{\mathbf{U}}_1 - \phi_1 \gamma_u \tilde{\mathbf{U}}_0)^\top (\mathbf{L}_1 - \mathbf{m}_{\delta_1} - \mathbf{V}_1 - \phi_1 \tilde{\mathbf{U}}_1 - \phi_1 \gamma_u \tilde{\mathbf{U}}_0)}{2\tau_{\psi_1}^2} \right\} \times \\ & \quad \exp \left\{ -\frac{\tilde{\mathbf{U}}_1^\top \mathbf{R}^{-1}(\rho_u, \kappa_u) \tilde{\mathbf{U}}_1}{2\sigma_{u,1}^2} \right\} \\ & \propto \exp \left\{ -\frac{\tilde{\mathbf{U}}_1 \mathbf{H}^\top \mathbf{H} \tilde{\mathbf{U}}_1 - 2\tilde{\mathbf{U}}_1^\top \mathbf{H}^\top (\mathbf{Y}_1 - \mathbf{m}_{\beta_1} - \gamma_u \mathbf{H}\tilde{\mathbf{U}}_0)}{2\tau_1^2} \right\} \times \\ & \quad \exp \left\{ -\frac{\phi_1^2 \tilde{\mathbf{U}}_1^\top \tilde{\mathbf{U}}_1 - 2\phi_1 \tilde{\mathbf{U}}_1^\top (\mathbf{L}_1 - \mathbf{m}_{\delta_1} - \mathbf{V}_1 - \phi_1 \gamma_u \tilde{\mathbf{U}}_0)}{2\tau_{\psi_1}^2} \right\} \exp \left\{ -\frac{\tilde{\mathbf{U}}_1^\top \mathbf{R}^{-1}(\rho_u, \kappa_u) \tilde{\mathbf{U}}_1}{2\sigma_{u,1}^2} \right\} \\ & \propto \exp \left[-\frac{1}{2} \left\{ \tilde{\mathbf{U}}_1^\top \left(\frac{\mathbf{H}^\top \mathbf{H}}{\tau_1^2} + \frac{\phi_1^2 \mathbb{I}_G}{\tau_{\psi_1}^2} + \frac{\mathbf{R}^{-1}(\rho_u, \kappa_u)}{\sigma_{u,1}^2} \right) \tilde{\mathbf{U}}_1 \right\} \right] \times \\ & \quad \exp \left[-\tilde{\mathbf{U}}_1^\top \left\{ \frac{\mathbf{H}^\top (\mathbf{Y}_1 - \mathbf{m}_{\beta_1} - \gamma_u \mathbf{H}\tilde{\mathbf{U}}_0)}{\tau_1^2} + \frac{\phi_1 (\mathbf{L}_1 - \mathbf{m}_{\delta_1} - \mathbf{V}_1 - \phi_1 \gamma_u \tilde{\mathbf{U}}_0)}{\tau_{\psi_1}^2} \right\} \right]. \end{aligned}$$

Thus, $\tilde{\mathbf{U}}_1 | \text{rest} \sim \text{MVN}(\mathbf{C}^{-1} \mathbf{b}, \mathbf{C}^{-1})$ where

$$\mathbf{b} = \frac{\mathbf{H}^\top (\mathbf{Y}_1 - \mathbf{m}_{\beta_1} - \gamma_u \mathbf{H}\tilde{\mathbf{U}}_0)}{\tau_1^2} + \frac{\phi_1 (\mathbf{L}_1 - \mathbf{m}_{\delta_1} - \mathbf{V}_1 - \phi_1 \gamma_u \tilde{\mathbf{U}}_0)}{\tau_{\psi_1}^2}$$

and

$$\mathbf{C} = \frac{\mathbf{H}^\top \mathbf{H}}{\tau_1^2} + \frac{\phi_1^2 \mathbb{I}_G}{\tau_{\psi_1}^2} + \frac{\mathbf{R}^{-1}(\rho_u, \kappa_u)}{\sigma_{u,1}^2}.$$

Full conditional distribution for $\tilde{\mathbf{V}}_0$

Note that $\tilde{\mathbf{V}}_0 \sim \text{MVN} \{ \mathbf{0}_G, \sigma_{v,0}^2 \mathbf{R}(\rho_v, \kappa_v) \}$. Then,

$$\begin{aligned}
& q(\tilde{\mathbf{V}}_0 | \text{rest}) \\
& \propto \mathcal{L}(\mathbf{L}_0 | \tilde{\mathbf{V}}_0, \text{rest}) \mathcal{L}(\mathbf{L}_1 | \tilde{\mathbf{V}}_0, \text{rest}) \pi(\tilde{\mathbf{V}}_0) \\
& \propto \exp \left\{ -\frac{(\mathbf{L}_0 - \mathbf{m}_{\delta_0} - \tilde{\mathbf{V}}_0 - \phi_0 \mathbf{U}_0)^\top (\mathbf{L}_0 - \mathbf{m}_{\delta_0} - \tilde{\mathbf{V}}_0 - \phi_0 \mathbf{U}_0)}{2\tau_{\psi_0}^2} \right\} \times \\
& \quad \exp \left\{ -\frac{(\mathbf{L}_1 - \mathbf{m}_{\delta_1} - \tilde{\mathbf{V}}_1 - \gamma_v \tilde{\mathbf{V}}_0 - \phi_1 \mathbf{U}_1)^\top (\mathbf{L}_1 - \mathbf{m}_{\delta_1} - \tilde{\mathbf{V}}_1 - \gamma_v \tilde{\mathbf{V}}_0 - \phi_1 \mathbf{U}_1)}{2\tau_{\psi_1}^2} \right\} \times \\
& \quad \exp \left\{ -\frac{\tilde{\mathbf{V}}_0^\top \mathbf{R}^{-1}(\rho_v, \kappa_v) \tilde{\mathbf{V}}_0}{2\sigma_{v,0}^2} \right\} \\
& \propto \exp \left\{ -\frac{\tilde{\mathbf{V}}_0^\top \tilde{\mathbf{V}}_0 - 2\tilde{\mathbf{V}}_0^\top (\mathbf{L}_0 - \mathbf{m}_{\delta_0} - \phi_0 \mathbf{U}_0)}{2\tau_{\psi_0}^2} \right\} \times \\
& \quad \exp \left\{ -\frac{\gamma_v^2 \tilde{\mathbf{V}}_0^\top \tilde{\mathbf{V}}_0 - 2\gamma_v \tilde{\mathbf{V}}_0^\top (\mathbf{L}_1 - \mathbf{m}_{\delta_1} - \tilde{\mathbf{V}}_1 - \phi_1 \mathbf{U}_1)}{2\tau_{\psi_1}^2} \right\} \exp \left\{ -\frac{\tilde{\mathbf{V}}_0^\top \mathbf{R}^{-1}(\rho_v, \kappa_v) \tilde{\mathbf{V}}_0}{2\sigma_{v,0}^2} \right\} \\
& \propto \exp \left\{ -\frac{1}{2} \tilde{\mathbf{V}}_0^\top \left(\frac{\mathbb{I}_G}{\tau_{\psi_0}^2} + \frac{\gamma_v^2 \mathbb{I}_G}{\tau_{\psi_1}^2} + \frac{\mathbf{R}^{-1}(\rho_v, \kappa_v)}{\sigma_{v,0}^2} \right) \tilde{\mathbf{V}}_0 \right\} \times \\
& \quad \exp \left\{ -\tilde{\mathbf{V}}_0^\top \left(\frac{\mathbf{L}_0 - \mathbf{m}_{\delta_0} - \phi_0 \mathbf{U}_0}{\tau_{\psi_0}^2} + \frac{\gamma_v (\mathbf{L}_1 - \mathbf{m}_{\delta_1} - \tilde{\mathbf{V}}_1 - \phi_1 \mathbf{U}_1)}{\tau_{\psi_1}^2} \right) \right\}.
\end{aligned}$$

Thus, $\tilde{\mathbf{V}}_0 | \text{rest} \sim \text{MVN}(\mathbf{C}^{-1} \mathbf{b}, \mathbf{C}^{-1})$ where $\mathbf{b} = \frac{\mathbf{L}_0 - \mathbf{m}_{\delta_0} - \phi_0 \mathbf{U}_0}{\tau_{\psi_0}^2} + \frac{\gamma_v (\mathbf{L}_1 - \mathbf{m}_{\delta_1} - \tilde{\mathbf{V}}_1 - \phi_1 \mathbf{U}_1)}{\tau_{\psi_1}^2}$ and $\mathbf{C} = \frac{\mathbb{I}_G}{\tau_{\psi_0}^2} + \frac{\gamma_v^2 \mathbb{I}_G}{\tau_{\psi_1}^2} + \frac{\mathbf{R}^{-1}(\rho_v, \kappa_v)}{\sigma_{v,0}^2}$.

Full conditional distribution for $\tilde{\mathbf{V}}_1$

Note that $\tilde{\mathbf{V}}_1 \sim \text{MVN}\{\mathbf{0}_G, \sigma_{v,1}^2 \mathbf{R}(\rho_v, \kappa_v)\}$. Then,

$$\begin{aligned}
& q(\tilde{\mathbf{V}}_1 | \text{rest}) \\
& \propto \mathcal{L}(\mathbf{L}_1 | \tilde{\mathbf{V}}_1, \text{rest}) \pi(\tilde{\mathbf{V}}_1) \\
& \propto \exp \left\{ -\frac{(\mathbf{L}_1 - \mathbf{m}_{\delta_1} - \tilde{\mathbf{V}}_1 - \gamma_v \tilde{\mathbf{V}}_0 - \phi_1 \mathbf{U}_1)^\top (\mathbf{L}_1 - \mathbf{m}_{\delta_1} - \tilde{\mathbf{V}}_1 - \gamma_v \tilde{\mathbf{V}}_0 - \phi_1 \mathbf{U}_1)}{2\tau_{\psi_1}^2} \right\} \times \\
& \quad \exp \left\{ -\frac{\tilde{\mathbf{V}}_1^\top \mathbf{R}^{-1}(\rho_v, \kappa_v) \tilde{\mathbf{V}}_1}{2\sigma_{v,1}^2} \right\} \\
& \propto \exp \left\{ -\frac{\tilde{\mathbf{V}}_1^\top \tilde{\mathbf{V}}_1 - 2\tilde{\mathbf{V}}_1^\top (\mathbf{L}_1 - \mathbf{m}_{\delta_1} - \gamma_v \tilde{\mathbf{V}}_0 - \phi_1 \mathbf{U}_1)}{2\tau_{\psi_1}^2} \right\} \exp \left\{ -\frac{\tilde{\mathbf{V}}_1^\top \mathbf{R}^{-1}(\rho_v, \kappa_v) \tilde{\mathbf{V}}_1}{2\sigma_{v,1}^2} \right\} \\
& \propto \exp \left[-\frac{1}{2} \left\{ \tilde{\mathbf{V}}_1^\top \left(\frac{\mathbb{I}_G}{\tau_{\psi_1}^2} + \frac{\mathbf{R}^{-1}(\rho_v, \kappa_v)}{\sigma_{v,1}^2} \right) \tilde{\mathbf{V}}_1 - \frac{2\tilde{\mathbf{V}}_1^\top (\mathbf{L}_1 - \mathbf{m}_{\delta_1} - \gamma_v \tilde{\mathbf{V}}_0 - \phi_1 \mathbf{U}_1)}{\tau_{\psi_1}^2} \right\} \right]
\end{aligned}$$

Thus, $\tilde{\mathbf{V}}_1 | \text{rest} \sim \text{MVN}(\mathbf{C}^{-1} \mathbf{b}, \mathbf{C}^{-1})$ where $\mathbf{b} = \frac{\mathbf{L}_1 - \mathbf{m}_{\delta_1} - \gamma_v \tilde{\mathbf{V}}_0 - \phi_1 \mathbf{U}_1}{\tau_{\psi_1}^2}$ and $\mathbf{C} = \frac{\mathbb{I}_G}{\tau_{\psi_1}^2} + \frac{\mathbf{R}^{-1}(\rho_v, \kappa_v)}{\sigma_{v,1}^2}$.

Full conditional distribution for $\sigma_{u,a}^2$ and $\sigma_{v,a}^2$ for $a \in \{0, 1\}$

Let the prior be $\sigma_{u,a}^2 \sim \text{Inverse-Gamma}(a_u, b_u)$. Then,

$$\begin{aligned}
& p(\sigma_{u,a}^2 | \text{rest}) \\
& \propto \left(\frac{1}{\sigma_{u,a}^2} \right)^{G/2} \exp \left\{ -\frac{\tilde{\mathbf{U}}_a^\top \mathbf{R}^{-1}(\rho_u, \kappa_u) \tilde{\mathbf{U}}_a}{2\sigma_{u,a}^2} \right\} \times \left(\frac{1}{\sigma_{u,a}^2} \right)^{a_u+1} \exp \left(-\frac{b_u}{\sigma_{u,a}^2} \right) \\
& \propto \left(\frac{1}{\sigma_{u,a}^2} \right)^{G/2+a_u+1} \exp \left\{ -\frac{\tilde{\mathbf{U}}_a^\top \mathbf{R}^{-1}(\rho_u, \kappa_u) \tilde{\mathbf{U}}_a / 2 + b_u}{\sigma_{u,a}^2} \right\}.
\end{aligned}$$

Therefore, $\sigma_{u,a}^2 | \text{rest} \sim \text{Inverse-Gamma} \left\{ \frac{G}{2} + a_u, \frac{\tilde{\mathbf{U}}_a^\top \mathbf{R}^{-1}(\rho_u, \kappa_u) \tilde{\mathbf{U}}_a}{2} + b_u \right\}$. A similar argument with using $\sigma_{v,a}^2 \sim \text{Inverse-Gamma}(a_v, b_v)$ produces a full conditional distribution

$$\sigma_{v,a}^2 | \text{rest} \sim \text{Inverse-Gamma} \left\{ \frac{G}{2} + a_v, \frac{\tilde{\mathbf{V}}_a^\top \mathbf{R}^{-1}(\rho_v, \kappa_v) \tilde{\mathbf{V}}_a}{2} + b_v \right\}.$$

Full conditional distribution for $\tau_{\psi_0}^2, \tau_{\psi_1}^2$.

Let the prior be $\tau_{\psi_a}^2 \sim \text{Inverse-Gamma}(a_\psi, b_\psi)$. Then,

$$\begin{aligned} p(\tau_{\psi_a}^2 | \text{rest}) &\propto \left(\frac{1}{\tau_{\psi_a}^2}\right)^{G/2} \exp\left\{-\frac{(\mathbf{L}_a - \mathbf{m}_{\delta_a} - \mathbf{V}_a - \phi_a \mathbf{U}_a)^\top (\mathbf{L}_a - \mathbf{m}_{\delta_a} - \mathbf{V}_a - \phi_a \mathbf{U}_a)}{2\tau_{\psi_a}^2}\right\} \times \pi(\tau_{\psi_a}^2) \\ &\propto \left(\frac{1}{\tau_{\psi_a}^2}\right)^{G/2+a_\psi+1} \exp\left\{-\frac{(\mathbf{L}_a - \mathbf{m}_{\delta_a} - \mathbf{V}_a - \phi_a \mathbf{U}_a)^\top (\mathbf{L}_a - \mathbf{m}_{\delta_a} - \mathbf{V}_a - \phi_a \mathbf{U}_a) / 2 + b_\psi}{\tau_{\psi_a}^2}\right\}. \end{aligned}$$

Thus, $\tau_{\psi_a}^2 | \text{rest} \sim \text{Inverse-Gamma}\left(\frac{G}{2} + a_\psi, \frac{(\mathbf{L}_a - \mathbf{m}_{\delta_a} - \mathbf{V}_a - \phi_a \mathbf{U}_a)^\top (\mathbf{L}_a - \mathbf{m}_{\delta_a} - \mathbf{V}_a - \phi_a \mathbf{U}_a) / 2 + b_\psi}{2}\right)$.

Full conditional distribution for τ_0^2, τ_1^2

Let the prior be $\tau_a^2 \sim \text{Inverse-Gamma}(a_y, b_y)$. Then,

$$\begin{aligned} p(\tau_a^2 | \text{rest}) &\propto \left(\frac{1}{\tau_a^2}\right)^{n/2} \exp\left\{-\frac{(\mathbf{Y}_a - \mathbf{m}_{\beta_a} - \mathbf{H}\mathbf{U}_a)^\top (\mathbf{Y}_a - \mathbf{m}_{\beta_a} - \mathbf{H}\mathbf{U}_a)}{2\tau_a^2}\right\} \times \left(\frac{1}{\tau_a^2}\right)^{a_y+1} \exp\left(-\frac{b_y}{\tau_a^2}\right) \\ &\propto \left(\frac{1}{\tau_a^2}\right)^{n/2+a_y+1} \exp\left\{-\frac{(\mathbf{Y}_a - \mathbf{m}_{\beta_a} - \mathbf{H}\mathbf{U}_a)^\top (\mathbf{Y}_a - \mathbf{m}_{\beta_a} - \mathbf{H}\mathbf{U}_a) / 2 + b_y}{\tau_a^2}\right\}. \end{aligned}$$

Thus, $\tau_a^2 | \text{rest} \sim \text{Inverse-Gamma}\left(\frac{n}{2} + a_y, \frac{(\mathbf{Y}_a - \mathbf{m}_{\beta_a} - \mathbf{H}\mathbf{U}_a)^\top (\mathbf{Y}_a - \mathbf{m}_{\beta_a} - \mathbf{H}\mathbf{U}_a) / 2 + b_y}{2}\right)$.

D Data sources of the covariates

Original data do not contain grid-level covariates, since grid cells are created in the analysis stage, not in the data-collection stage. Therefore, to keep site-level and grid-level covariates on the same scale, simultaneously at the coordinates of each survey site and each centroid of the grid cell, we extract the values of the aforementioned covariates from various data sources. Distances to the shoreline are calculated by the great circle distance between survey points or grid centroids and the seashore. The coordinates for seashore are available using the high resolution shoreline layer of the Global Self-consistent, Hierarchical, High-resolution Geography (GSHHG) Version 2.3.7 (Wessel and Smith, 1996). For depth values, they are extracted using AusBathyTopo (Australia) 250 m 2023 - A High-resolution Depth Model (Beaman, 2023). For the mean level of chlorophyll a and the minimum sea surface temperature, the values are extracted from

BIO-ORACLE (Tyberghein et al., 2012), which represent the monthly average values for the years 2002-2009. Human population within 100 km radius of each survey point and grid cell is calculated by using the Socioeconomic Data and Application Centre (SEDAC) Gridded Population Of The World database for the year 2000 (CIESIN, 2018). Distances to the market are the great circle distance between the survey points or grid centroids and the nearest provincial or national capital, where the coordinates are identified from the World Cities base map layer (ESRI, 2023). The habitat types at the survey sites are brought from the original MPA data, while the habitat types at the grid cells are matched with those of the nearest survey sites.

E Sensitivity to the resolution of grid cells

To check the sensitivity of the marginal posterior distributions of Δ according to the grid cell resolution, we fit the proposed model with coarser and finer resolutions. For coarser resolutions, we cover the spatial domain with grid cells 1.0×1.0 degree², while we use grid cells 0.6×0.6 degree² for finer resolution. The number of grid cells with the coarser resolution is $G = 293$, while that with the finer resolution is $G = 813$. We use the same prior distributions as described in Section 5.2, except that we assign $\log(\rho_u)$ and $\log(\rho_v)$ with $\text{Normal}\{\log(400), 0.5\}$ for the coarser resolution. The posterior mean of Δ with the resolution used in the main manuscript is 0.71 with the 95% credible interval being $(-0.24, 1.71)$. Similarly, those with coarser and finer resolutions are 0.343 and 0.960, respectively, while the 95% credible intervals are $(-0.858, 1.652)$ and $(-0.358, 2.191)$ respectively.